NASA CONTRACTOR REPORT

NASA CR-1506

NASA CR-1506
c. 1

RADIO ASTRONOMICAL STUDIES WITH 1500-METER DIAMETER LOW-FREQUENCY TELESCOPE

by M. R. Kundu

Prepared by
ASTRO RESEARCH CORPORATION
Santa Barbara, Calif.
for Goddard Space Flight Center

NATIONAL AERONAUTICS AND SPACE ADMINISTRATION • WASHINGTON, D. C. • JANUARY 1970

RADIO ASTRONOMICAL STUDIES WITH 1500-METER DIAMETER LOW-FREQUENCY TELESCOPE

By M. R. Kundu

Issued by Originator as Technical Note No. ARC-LTN-2

Prepared under Contract No. NAS 5-11596 by
ASTRO RESEARCH CORPORATION
Santa Barbara, Calif.

for Goddard Space Flight Center

NATIONAL AERONAUTICS AND SPACE ADMINISTRATION

For sale by the Clearinghouse for Federal Scientific and Technical Information
Springfield, Virginia 22151 – Price $3.00

RADIO ASTRONOMICAL STUDIES WITH 1500-METER DIAMETER LOW-FREQUENCY TELESCOPE

INTRODUCTION

Observations in the radio frequency portion of the electromagnetic spectrum have provided astronomers with information that has great promise of yielding much better understanding of the universe. The recently discovered "pulsars" are an example of new phenomena. Closer to home, the study of solar radio bursts at metric and decametric wavelengths during the last solar maximum has provided important information about the physical conditions in the sun's outer corona. For example, observations of certain solar bursts have made it possible to determine electron densities in coronal streamers out to about 3 solar radii from the center of the sun. The electron density in coronal streamers at this level corresponds approximately to a plasma frequency of 20 MHz, which is close to the average ionospheric cutoff. To study the properties of solar bursts at lower frequencies, and therefore to determine electron density at greater distances from the center, it is necessary to make observations from above the ionosphere. The same is true for low-frequency phenomena for other radio sources.

The observable radio spectrum can be extended to frequencies well below the ionospheric cutoff by means of spaceborne experiments such as those currently used for the OGO and RAE spacecraft. The intensity variations of low-frequency solar bursts as a function of time and frequency, as obtained from such experiments, will certainly lead to valuable information on the solar corona, galactic sources, and the interplanetary and intergalactic media. However, the necessary simplicity of the antennas will impose severe limitations on the spatial resolution attainable. Consequently, very little can be learned about the size, brightness distribution, and motion of the burst sources, and difficulty will be encountered in discriminating between solar and various other sources.

The resolution of radio telescopes has always been the most important limiting factor in the observation of radio sources. The resolving power of a telescope is determined by the ratio of the wavelength of observation to the diameter of the telescope. Taking a typical optical wavelength, 5×10^{-5} cm, and a typical radio wavelength, 5×10^{2} cm, it is apparent that an aperture

must be of the order of 10^7 times as wide to give the same resolution at radio wavelengths as at optical wavelengths. It must have dimensions of hundreds of kilometers to rival even the moderate size optical telescopes. The difficulty and cost of constructing such enormous continuous-aperture radio telescopes are prohibitive even on the ground, and in space where the wavelengths employed are even longer, the problems become insurmountable.

Fortunately, however, a great deal of information can be obtained with lower resolution devices inasmuch as radio sources are usually quite energetic and often quite "large" in the sense of the necessary resolution angle. For example, there is evidence that some well-known types of solar bursts go down at least to 600 KHz (the plasma frequency for an electron density of 4.6×10^3 cm^{-3}). A rough model of the outer solar corona estimated from optical zodiacal light observations (see Fig. 1) gives 600 KHz as a coronal plasma frequency at about 12 solar radii (3° subtended at the earth) from the center of the sun. In addition, the burst sources are likely to subtend an arc of about 1° at such long hectometric wavelengths.

A technology development program is being conducted by NASA Goddard Space Flight Center to create the technical knowhow to support the design of an orbiting "Low Frequency Radio Telescope" henceforth identified as LOFT (see Ref. 1). The large size (approximately one mile) of this radio astronomy research tool arises from the desirability to study with good resolution the low frequency (0.5 to 10 MHz) radio emissions that do not penetrate the earth's ionosphere. An artist's rendition of the LOFT is shown in Figure 2. It consists of a nearly paraboloidal reflector of very large size (1500-meter aperture was selected for detailed study) which is composed of a tenuous network of conducting ribbons. The configuration is launched into a high orbit (~6000 km) in a tightly packaged state. Deployment and centrifugal stiffening are achieved by spinning about the axis of symmetry. A deployable central compression column forms the spine of the vehicle and connects the base of the paraboloid to the broad-band feed at the focus. The column also reacts tension loads in the front stays which pull the reflector into shape. Pointing of the radio telescope is achieved by circulating currents around the net and interacting with the geomagnetic field.

As presently conceived, the LOFT (1500 meters diameter) will operate in two modes: simple telescope mode and interferometer

mode. In the simple telescope mode it will have a pencil beam of about 3° x 3° at 4 MHz, and 1° x 1° at 10 MHz. This resolution, though not as good as might be desired, will be useful for certain studies of solar bursts. For example, even with a 4° beam, one should be able to determine the position of sources to an accuracy of about 20' arc, which is adequate in view of the fact that burst sources are likely to be of larger size. The positions thus determined, when combined with a proper interpretation of the generating mechanisms of certain radio bursts, could lead to determinations of electron density in the outer corona out to distances of the order of 50-100 solar radii.

It is obvious that the same basic instrument will also yield information on the spatial distribution of discrete radio sources including external galaxies, gaseous nebulae, supernova remnants, etc.

The collecting area of LOFT will be of the order of 10^6 square meters, and therefore it should yield information on the brightness and position of a large number of radio sources. While resolutions of several degrees cannot be considered very good on the basis of present-day standards for galactic and extragalactic research, the situation is roughly the same as existed some ten years ago at meter wavelengths.

In the following sections some of the radio sources are discussed in detail and the usefulness of the LOFT instrument assessed.

STUDY OF SOLAR RADIO BURSTS

We shall first review our knowledge of solar radio emissions and then discuss possible experiments that can be done at low frequencies by means of LOFT.

Solar radio emission can be divided broadly into three categories. The radio emission from the quiet sun - that is, the emission that arises from the solar atmosphere in the absence of any active region. It is caused by free-free transitions of electrons in thermodynamic equilibrium; it has a black-body spectrum - that is, it dies away toward longer wavelengths (meter and decameter wavelengths). Consequently in the regions of the radio spectrum which are of interest to LOFT, the quiet sun emission may not have much importance. This is even more so since the strong galactic background that is observed at low frequencies will make the contrast between the sun and galactic background become less prominent. The second component of solar radio emission is the slowly varying component. This component is closely associated with sunspots, and plage regions as observed at optical wavelengths. It appears and disappears in fairly close agreement with the latter and is also correlated well with the time variable part of the drag experienced by earth satellites in the outer atmosphere of the earth. The spectrum of the slowly varying component has a maximum around 5-6 cm wavelength and decreases sharply toward both millimeter and meter wavelengths. It has not been observed below about 150 MHz. Obviously this component presents no interest for LOFT observations.

The different kinds of solar bursts, on the other hand, have a spectrum which generally increases toward low frequencies. Consequently, these transient emissions will be of great interest when observations can be made from beyond the earth's atmosphere. As the frequencies on which burst radiation occurs are related to the electron density in the corona at the region of origin, any observations of bursts at LOFT frequencies will refer to coronal regions further out from the sun than can be studied at present. Such observations are expected to yield information about the expulsion of particle clouds and magnetic fields from the chromosphere at times of solar flares. One pictures the ejection of swarms of energetic particles carrying magnetic field with them on their passage up through the corona and either carrying on into interplanetary space or being retained at high levels and slowly dissipating their energy by radio frequency emission

caused by spiraling in the field. A great deal is known regarding the ejection phase, but we know very little about the trapping that takes place at higher levels and the leakage or direct escape of particles into interplanetary space. This trapping phase, with special reference to the structure and evolution with time will be particularly interesting for LOFT.

The quiet sun radiation, although dominated by storm and burst radiations, may be an interesting topic for investigation, particularly at times when the sun passes in front of the Milky Way and acts as an obscuring ball of lesser brightness than the background sky. At other times, the image of the galaxy, much diminished, will appear reflected in the outer corona. It is quite possible that interesting properties of the solar outer corona will be revealed by observations of the effects on the galactic background caused by the sun over a range of low frequencies. This may well be a method of monitoring the transient effects of solar flares by recording galactic noise as it propagates through the sun's corona. The sun's activity, as we know, influences the interplanetary plasma, especially the irregularities of its electron density and magnetic field. One way of monitoring this activity is through observing the interplanetary scintillations of small-diameter extragalactic sources. It is quite likely that this phenomenon as observed on LOFT frequencies will be a very good indicator of this activity, and consequently of solar wind.

Solar Bursts

As mentioned earlier, the most obvious solar study that can be done with LOFT is the study of solar bursts. Solar radio astronomy was started in 1942 with the discovery by Hey of intense nonthermal solar radio emission at meter wavelengths, and by Southworth of thermal radiation from the sun at centimeter wavelengths. However, because of the war, not much was done until 1946. During the maximum of solar activity (1947-48) which followed this discovery, only isolated observations were taken since not many instruments were available for observing the sun systematically. However, these observations were helpful for the development of appropriate instruments for solar studies during the next solar maximum. Systematic observations made during the last solar cycle have greatly improved our knowledge of solar physics and have, in a way, revolutionized our understanding of solar-terrestrial relationships. These observations and their interpretations have been summarized in several reviews (e.g.,

Ref. 2) and in a comprehensive book on solar radio astronomy (Ref. 3). It is quite clear that as a result of 20 years research, we have a fairly consistent physical picture of the radio sun at meter and centimeter wavelengths. But our knowledge at the two ends of the solar radio spectrum, millimeter and decameter-hectameter wavelengths, is not adequate. In particular, because of lack of high resolution observations, the nature of the sources of the slowly varying component and of bursts at millimeter wavelengths is relatively unknown. For the same reason, we know very little of the position, motion, and structure of burst sources at decameter and hectameter wavelengths, particularly as a function of frequency. Even at meter wavelengths where systematic and extensive observations have been made, the nature of burst sources does not seem to be fully understood. Indeed, recent two-dimensional observations (solar maps) taken rapidly (1 per second) with a resolution of 3' arc by the Australian radioheliograph (Ref. 4) have demonstrated that fast phenomena in the sun's upper corona may originate from several regions simultaneously, and they occur in such a manner as to suggest some kind of magnetic linkage between different regions situated at widely separated locations on the sun. There is obviously a need for the production of similar, fast, two-dimensional maps at both millimeter and decameter-hectameter wavelengths. However, the solar phenomena that occur at millimeter wavelengths are not nearly as fast as at meter wavelengths, and so one can be content with two-dimensional maps taken at a slower rate. Of course, at decametric-hectametric wavelengths one should ideally have rapid two-dimensional maps. However, any kind of image synthesis or picture-taking instrument is quite involved. On the other hand, a great deal can be understood regarding the physical nature of the sources of fast phenomena and consequently of plasma instabilities in the upper corona from an intensive study of decameter-hectameter wavelength active regions simultaneously at a number of frequencies. These are precisely the studies for which the LOFT can be quite suitable.

The bursts at meter and decameter wavelengths are characterized by great variety and complexity. They are classified into five types, principally on the basis of their spectral characteristics: type I, or storm radiation characterized by slowly varying, continuous radiation with superposed short-lived narrow-bandwidth bursts; drifting bursts of type II and type III; long lasting continuum bursts of type IV; and short-lived continuum bursts of type V. The dynamic spectra of these bursts in the frequency-time domain are illustrated in Figure 3. All such bursts with the exception of a minority of type I bursts are

associated with solar flares.

Type I, or noise storm radiation, consists of a slowly varying broad-band enhancement of the continuous solar radiation, lasting from a few hours to a few days, on which are superimposed series of narrow-band ($\sim$ 5 MHz) bursts (type I), each of which lasts from a fraction of a second to a few seconds. The radiation is strongly circularly polarized, and the onset of the bursts may occur in association with flares or with the appearance of visible active regions on the solar disk.

Type II and type III bursts are intense events of minutes' and seconds' duration, respectively. Their spectra consist of emission features that drift toward lower frequencies at rates of about 1 MHz/sec and 20 MHz/sec, respectively. It is remarkable that these are the only two distinct narrow-range-of-drift-rate values observed on meter wavelengths. These drifting bursts are interpreted to be due to plasma oscillations at the local plasma frequency, and this interpretation has been supported by directional observations. The plasma frequency depends on the electron density that decreases with height in the solar atmosphere. Thus, on the assumption of a model electron density distribution, the two characteristic drift rates imply the existence of two distinctive types of bursts, "slow drift" and "fast drift", whose exciting sources travel outward through the solar atmosphere with velocities of about 1000 km/sec (type II) and 100,000 km/sec (type III). Second harmonics are observed in many cases.

Type IV burst is a partially polarized, smooth continuum emission, occurring over a very wide range of frequencies between centimeter and decameter waves and lasting from about 10 minutes to a few hours. Wide differences in the characteristics of type IV events on different wavelengths suggest that they originate from different sources. The type IV source on meter waves generally has a large angular size and an initial transverse velocity of about a few thousand km/sec.

The type V burst is a similar continuum event that lasts only from a few seconds to a few minutes and is nearly always limited to meter waves.

Figure 4 shows the spectra of strong radio bursts and continuum storms in relation to those of the quiet sun and the slowly varying component. The phenomenology of different flare-associated bursts can be described as follows.

Almost simultaneously with the explosive phase of the Hα flare there is a sudden release of about 10^{35} or so electrons, possibly in various directions. Some of these electrons move down to the trapping region and are accelerated by the Fermi mechanism in the active region that contains the sunspot magnetic field and has a density several times the coronal density. They can attain energies up to 500 KeV or higher, provided that mechanical energy in the form of shock waves is also released from the flare explosion. The fast electrons produce the impulsive burst on centimeter waves by nonthermal bremsstrahlung and synchrotron mechanism and the very high-energy x-ray burst by nonthermal bremsstrahlung. Simultaneously with the downward moving electron streams, a stream of accelerated electrons is also ejected upward. This stream of high-energy particles travels along coronal streamers with velocities of 10^5 km/sec and excites longitudinal plasma oscillations successively at different levels of the coronal plasma, which after being transformed into transverse EM waves by scattering on density and charge fluctuations, are observed as type III bursts. Following the collapse of an important flare, a cloud of gas with a hydromagnetic shock front is also ejected. This cloud of gas with the magnetohydrodynamic shock front ahead of it also travels along a coronal streamer with velocities of 1000 km/sec and, on reaching coronal regions of sufficiently low density ($f_p \sim 100$ MHz) and low collision frequency (1 Hz), excites longitudinal plasma oscillations successively at different levels in the corona. These longitudinal plasma waves converted into transverse electromagnetic radiation by Rayleigh and combination scattering at density and charge fluctuations in the coronal plasma are observed as type II bursts. Part of the same shock wave propagates into the chromosphere and is responsible for the acceleration of electrons and protons. Some of the accelerated protons are capable of overcoming the trapping magnetic field and are therefore observed as ground-level cosmic ray increases. The accelerated electrons remain trapped and radiate synchrotron radiation which is observed as centimeter and decimeter wavelength type IV.

The late phase of large flares also indicates the existence of large clouds of electrons trapped within the sunspot magnetic fields both in the chromosphere as well as in the corona out to several solar radii. These are the electrons responsible for type IV continuum radiation, which occurs in three distinct phases. The first phase, or type IV A, occurring on centimeter and decimeter wavelengths is due to synchrotron radiation of electrons released during the flare, subsequently accelerated by a Fermi-like mechanism and trapped in the sunspot magnetic field at low

altitudes of the chromosphere. The second phase, or "moving" type IV (type IV B) occurring on meter and decameter waves is also synchrotron radiation from relativistic electrons high in the corona. The necessary magnetic field may be the sunspot magnetic field or a frozen-in magnetic field carried by the flare-ejected plasma cloud to higher altitudes. The number of electrons required for this emission is of the order of 100 cm^{-3} of 1 MeV energy, assuming a magnetic field of several gauss in the corona. The energy of the electrons radiating type IV A in the stronger sunspot magnetic field at lower altitudes ranges from a few hundred KeV to 1 MeV. The third phase of "stationary" type IV (type IV C and continuum storm) appears to be due to Cerenkov plasma radiation. It has been suggested that high energy particles ejected and accelerated during the flare would remain trapped near the sun in magnetic configurations probably associated with coronal streamers. With the gradual weakening of the magnetic field, these energetic particles slowly diffuse into the streamers and excite Cerenkov plasma waves which transfer part of their energy directly to electromagnetic waves. At a still later stage of the flare, the type IV C and continuum storm degenerates into an ordinary noise storm.

Extension of solar radio bursts to low frequencies. - Drifting bursts of type II and type III, and continuum bursts of type IV are expected to extend below 20 MHz. As revealed by the RAE data (Ref. 5) by far the most frequently occurring type of burst at low frequencies is the type III burst. Another category of bursts - type IV - is also likely to be frequently observed during solar maximum because of the very nature of the generating mechanism, that is, from energetic particles stored in regions far in the outer corona.

Type III bursts. - Type III bursts have been detected by the sweep frequency receivers aboard the Alouette and RAE-A satellites and have been found to extend with apparently undiminished intensity down to as far as 550 KHz, which is the lower frequency limit of the RAE equipment. In type III bursts, there is a rapid drift of the frequency of maximum intensity toward lower frequencies at a rate of about 20 MHz/sec at 100 MHz. The rate decreases at lower frequencies. It is generally believed that type III bursts are plasma oscillations excited by a stream of electrons moving outward from the vicinity of an active region in the lower atmosphere of the sun. The frequency of maximum intensity at a particular instant would therefore be the plasma frequency corresponding to the level reached by the source in its progress outward.

Consequently, from a comparison of measured source positions and frequency drift rates one can determine electron density profile in the corona. High frequency observations indicate that electron densities in the outer corona are roughly an order of magnitude higher than that expected from extrapolating optical measurements beyond about 2 solar radii. This can be explained by postulating that the disturbances which lead to solar bursts travel out from active regions along coronal streamers in which the electron densities are an order of magnitude higher than in the ambient corona.

Studies of type III bursts have been conducted at many frequencies in the metric and decametric range so that the electron density distribution in streamers over active solar regions out to about 3 solar radii has been fairly well determined. Figure 5 presents a review of what is known about the electron density profile in the corona (Ref. 6). The shaded areas marked "pole" and "equator" indicate the range of optical eclipse observations of the coronal electron density over those regions. The solid curves show the models of van de Hulst derived from eclipse observations, whereas the broad shaded area near the top of the field labeled "streamer" represents the error limits of determinations based on type III (dots) and type II bursts (crosses). The short solid curve is Newkirk's streamer model based on optical coronameter observations, and the dashed curve and small shaded area nearby give Hepburn's and Schmidt's optical eclipse measurements of streamers. The long solid curve is van de Hulst's equatorial maximum model increased by a factor of ten.

Directional observations made with LOFT are likely to extend the electron density profile out to roughly 50 - 100 solar radii. This extension will be of utmost importance from the point of view of solar physics and solar-terrestrial physics. By direct measurements of physical conditions from satellites and space probes, the interplanetary medium near the earth's orbit can be explored. However, the region out to 50 solar radii (1/4 the distance to the earth) can be investigated only indirectly. It appears that the LOFT solar burst observations will offer a fruitful approach, providing information on positions of burst sources at successive frequencies and consequently on velocities of type III bursts. This, together with the measured frequency drift rate, will yield the electron density profile in the outer solar corona.

In addition, the LOFT observations will give data on the size and brightness distribution of solar bursts, which may be directly related to density fluctuations in the corona at angles

not accessible to ground-based equipments.

Observations of decametric wavelengths have shown that type II, III, and IV bursts do not have simple gaussian shapes; their brightness distributions can be approximated by the sum of a wide gaussian "halo" and a narrow "core". In the case of type III bursts, the relative sizes and intensities of the two components change with time and frequency, suggesting that the halo is produced by scattering in the corona about the true source, which has an angular size no larger than that of the core. The scattering apparently is due to irregularities or fluctuations in the electron density. Observations at decametric wavelengths give an angular size of 38' for a type III halo and $\leq$ 10' for the core; the ratio of power in the core to total power is 8 percent. Other types of solar bursts have similar brightness distributions at the same wavelength. Such brightness distributions are definitely observable with LOFT even with a beam of 2° - 3°.

Comparison of the brightness distributions of solar bursts at hectometric and kilometric wavelengths with those at decametric wavelengths will provide data on the bursts themselves and also on the structure of the interplanetary medium. According to simple scattering theory, the variation with wavelength of the angular size, Φ , of the halo of scattered radiation is given by

$$\Phi \propto \lambda^2 \, \Delta N \, n^{\frac{1}{2}}$$

where ΔN = electron density fluctuation

n = number of irregularities along line of sight.

Since $n^{\frac{1}{2}}$ does not change appreciably over large distances in the corona, it can be treated as a constant. Little is known about the variation of ΔN with ρ , the distance outward in the corona (measured in units of the solar radius). Most investigators have assumed that $\Delta N \propto N$, the electron density at a particular point in the corona. At the plasma level, the plasma frequency and therefore the corresponding electron density is inversely proportional to λ^2 . Consequently, for bursts of types II and III which involve plasma oscillation, Φ should remain constant as the wavelength increases if Φ is entirely due to scattering. In the case of bursts which involve other kinds of generating mechanisms such as synchrotron radiation as is invoked for

broad-band "moving" type IV, the angular size should vary as the square of the wavelength.

Observations of type III bursts from the ground down to frequencies of 5 or 6 MHz have shown that the numbers of bursts observed does not decrease appreciably as one moves from the center of the disk to the limb. This is in direct contradiction to the theory of ray-propagation in the corona, and the effect is generally ascribed as due to scattering at electron density irregularities. In order to determine the effect of ray propagation at low frequencies, one can trace the paths of rays at say 1 MHz (Fig. 6) coming from various directions as they traverse the corona on their way to the earth. The model for the electron density distribution in the corona used in these computations was the following:

$$N = 6.75 \times 10^6 \rho^{-3}(1 + 15 \rho^{-3}) \qquad 2 \leq \rho \leq 50$$

where ρ = the distance from the center of the sun, measured in solar radii.

This model results from a combination of the models of Baumbach, revised by Allen (Ref. 7),

$$N = 1.55 \times 10^8 \rho^6 (1 + 1.93 \rho^{-10}) \qquad \rho \geq 1$$

and Ingham (Ref. 8)

$$N = 6.75 \times 10^6 \rho^{-3} \qquad 6 \leq \rho \leq 50$$

In Figure 6, the earth is at the top, and the scale is indicated by the dark spot in the center representing the photosphere of the sun with a radius of 700,000 km. The plasma level corresponding to the frequency is indicated by the "ambient plasma level" circle. In coronal streamers, along which type II and III bursts appear to travel, the electron density is assumed to be one order of magnitude higher than the "ambient" electron density. The plasma level in streamers is shown by the outer circle. Extending toward the bottom is the "cone of avoidance",

from which no rays can reach the earth. The point of intersection of this cone with the streamer plasma level indicates that type II and III bursts should continue to be observed over the whole forward hemisphere of the sun, rather than from the center alone. Therefore, it is expected that observation of bursts due to plasma oscillations (types II and III) will be possible at the limb. Since the burst sources tend to travel radially outward, the motion of the limb bursts is roughly perpendicular to the line of sight and therefore can be detected and measured more easily by the LOFT. It will be of interest to see if low-frequency plasma bursts are observed even when the active region is beyond the limb, for example, due to coronal scattering.

Type II bursts. - Type II (slow-drift) bursts are the most intense events recorded at metric and decametric wavelengths. They occur much less frequently than type III bursts; the rate near solar maximum is about one burst per 50 hours. They occur in association with large optical flares, beginning from 5 to 20 minutes after the start of the flare and drifting to low frequencies at a rate of about 1 MHz/sec or less. The spectral features at a particular frequency often occur simultaneously at a frequency twice as high, i.e., radiation occurs at the fundamental and first harmonic. Measurements of source positions indicate that the exciting disturbance moves outward through the corona as in the case of type III bursts, but at a velocity 20 to 50 times lower. The generating mechanism is again plasma oscillations, but in this case the exciting agency is assumed to be a shock front originating near the position of the flare, that moves out at a velocity of about 1000 km/sec through the corona. Type II bursts have been observed down to 7 MHz (Ref. 18) from the ground. Hartz (Ref. 9) was unable to identify positively any bursts except type III on the Alouette records because of the shortness of the recording interval and the satellite spin modulation, but he believes that parts of some type II bursts were recorded at times when ground-based observatories reported them at higher frequencies.

LOFT observations of type II bursts at frequencies down to 500 KHz can be used in the same way as those of type III bursts to determine the electron density profile in the corona. The plasma clouds that are ejected at the time of flares and that eventually travel out through the corona, with a shock front associated with it, move at the same velocity as type II bursts,

and impinging on the earth's magnetosphere produce geomagnetic storms. Observing these bursts at great distances from the sun with LOFT should greatly improve our understanding of the interaction of solar plasma clouds with the earth's magnetosphere.

Type IV bursts. - The type IV burst at metric and decametric wavelengths consists of a broad, intense continuum radiation that follows about 20 percent of the large solar flares that produce type II bursts. Thus the type IV burst is an even rarer phenomenon than type II. Figure 7 shows the number of type IV bursts per six-month interval during the past solar cycle. If the last solar cycle is a fairly representative one, then the launching of the full-scale LOFT in 1980 or 1981 would provide maximum opportunity to record type IV bursts at low frequencies. These bursts are strongly associated with solar proton events and their further study will greatly improve our understanding of their generating mechanism as well as how the radio-emitting electrons and the low-energy protons are stored near the sun and in the interplanetary medium.

Some of the sources of type IV have been observed to travel at velocities of 1000 km/s or more, sometimes out to distances of 6 or 7 solar radii while others remain fixed. A type IV burst can last from an hour to a day or longer, although the moving phase usually lasts no longer than an hour. The intensity, large size, motion and low directivity, and circular polarization of moving type IV are explained in terms of synchrotron radiation from energetic electrons trapped in coronal magnetic fields.

Immediately after the flare explosion, energetic particles - protons and electrons - are ejected; simultaneously a plasma cloud that is formed as a part of the shock front that generates type II bursts propagates downward into the solar chromosphere and helps in accelerating the electrons and protons still further. Some of the accelerated electrons and protons are carried with the plasma cloud which moves through the outer corona and radiates synchrotron radiation at meter and decameter wavelengths in the frozen-in-magnetic field of the ejected plasma cloud.

As we know, type IV bursts (including continuum storms) are closely associated with solar protons and with geomagnetic storms. It is believed that low-energy protons are stored in the vicinity of the sun, in magnetic configurations probably

associated with the coronal streamers (Fig. 8). The continuum storm is the only flare-associated radio event that has a time scale similar to that of the low-energy solar protons. It has been suggested that these storm regions (Ref. 10) may be related to the regions where low-energy solar protons are stored. Observations of this continuum storm on low frequencies will help determine the location of these regions out to altitudes of the order of 50 to 100 solar radii and, with simultaneous observation of cosmic rays, may ultimately lead to the identification of storm regions as the regions where low energy solar cosmic rays are stored.

The interpretation of type IV bursts in terms of gyrosynchrotron radiation from energetic electrons in the sun's magnetic field requires the detailed understanding of the generation and propagation of radio waves in a plasma. Indeed, it has been shown that the low-frequency cut-offs sometimes observed in the spectra of type IV bursts could be interpreted as due to the suppression of synchrotron emission due to the influence of the ionized medium. This interpretation, if correct, can lead to fairly good estimates of the coronal magnetic field and the range of electron energies involved in the emission (Ref. 11). Obviously, then, the study of the low-frequency spectra of type IV bursts, especially on decameter-hektameter waves, will be quite valuable.

Important information can be obtained on the solar corona from a study of the characteristics of type III bursts on low frequencies. As discussed earlier, the type III bursts result from excitation of plasma oscillations by particle streams at successively higher levels in the corona. The damping of plasma oscillations is mainly caused by collisions between electrons and protons and hence the rate of decay of type III bursts should correspond to the collision frequency at the appropriate height in the corona. Assuming that the radiation arises at or near the plasma frequency, the collision frequency can be directly related to the electron temperature and thus the measurement of decay rate can result in the determination of coronal temperature. Such measurements over a wide range of frequencies can give the temperature gradient in the corona. Further, by studying the rate of rise of an individual burst over a wide range of frequencies as it penetrates further out into the corona, it may be possible to determine the dispersion of the particle stream causing the type III plasma oscillations. In addition, one may be able to understand better the nature of the exciting agency.

STUDY OF GALACTIC AND EXTRAGALACTIC SOURCES

Galactic radiation comes both from broad structural components of the galaxy and from galactic objects such as supernova remnants and gaseous nebulae.

Some observations on the galactic background have been made by the Michigan and Goddard groups. However, no general mapping of the galaxy exists, as yet, so LOFT can be valuable in this respect. This mapping should reveal discrete sources in the galaxy - HII regions and supernova remnants. While the resolution available may not be adequate for revealing any structural details within the discrete sources, careful measurement of the total flux density can lead to important information relating to the physics of these objects. For example, in HII regions, the availability of a low frequency point in the total spectrum should lead to a better determination of the electron temperatures in these regions. For supernova remnants having shell structure, the total flux densities at low frequencies in the shell-part of the sources can throw considerable light on the mechanism of generation of radio waves - whether the energetic electrons emitting synchrotron radiation originated during the supernova explosion or they were swept over along with the galactic magnetic field by the shock wave associated with the expanding supernova envelope.

Supernova remnants, such as Taurus-A and Cassiopeia-A, have been observed to the limits of ionospheric cut-off and the shape of the spectra at low frequencies should obviously be of considerable interest. From the energy spectrum of the electrons emitting synchrotron radiation, one can show that the emission must fall off as low frequencies are approached. However, the details of this fall-off (Ref. 16) have never been observed; obviously, such spectral observations at low frequencies should greatly help in our understanding of the nature and evolution of supernova remnants.

Accurate flux density determinations at low frequencies (1 - 10 MHz) of HII regions in the galaxy can lead to correct estimates of their electron temperatures. As we know, the brightness temperature of a HII region depends upon whether

the region is optically thin or thick.* Now, T_b is first observed at a high frequency where the plasma is optically thick. Then the radio spectrum is computed for different assumed electron temperatures, and the predicted spectrum is compared with the actually observed spectrum. The lowest frequency that has been used so far for this kind of electron temperature determination is 41 MHz with the 1000 ft. diameter spherical telescope of Arecibo. An example of such determination is shown in Figure 9 (Ref. 17). It is quite clear that the presently determined values of flux density at low frequencies are not accurate enough, and so accurate low-frequency values will help determine better values of electron temperatures. One will be able to confirm whether the lower temperatures of Orion A and NGC 2024 determined in this manner are actually a consequence of the variation of T_e as a function of distance from the central exciting star. Alternately, the lower temperatures could refer to the outer layers of Orion A and NGC 2024, in which case the flux-density values obtained at low frequencies from space vehicles should refer to still outer layers of the HII regions.

Another use of low-frequency observations of gaseous nebulae lies in studies relative to galactic structure. The galaxy looks like a radio-emissive band stretched along the Milky Way and its emission comes from the entire galaxy. As low frequencies are approached, the local gaseous nebulae will obscure the distant galactic radiation. At a temperature of 10^4°K, these thermal objects will appear dark, since the background is very bright. At lower frequencies than have yet been observed, even relatively tenuous hydrogen clouds will become opaque and will then reveal their distribution about us in space. Most of these clouds should be concentrated in spiral arms of the galaxy, and since the formation of galactic spiral structure is still not fully understood it will be useful to have data on the distribution of such clouds from low-frequency observations. The spiral arms are thought to be confined to a flattened radio-emissive disk which again is enveloped by a spherical halo within which relativistic electrons emit by the synchrotron process. The halo is thought to be the source of galactic cosmic rays; however,

---

* $\left[T_b = \int_0^{\tau} T_e e^{-\tau'}\, d\tau' \right.$; for constant T_e, $T_b = T_e(1-e^{-\tau}) = T_e$ for $\tau \gg 1$ and $= \tau T_e$ for $\left. \tau \ll 1 \right]$

recent observations indicated that the halo is not as large as originally thought. Consequently, it would be valuable to extend the observations of the halo to lower frequencies - with particular reference to determining the energy spectrum and density of electrons.

Extragalactic Sources

In the following pages we shall review our knowledge of extragalactic sources from ground-based observations at low frequencies with a view to understanding their physical nature.

Observations of discrete radio sources at frequencies below 20 - 30 MHz from the ground can only be made near the time of minimum solar activity since the terrestrial ionosphere blocks radio waves from outside. During the most recent solar minimum (1963-1965), a number of groups have made observations at low frequencies. These observations have provided information on the spectral behavior of a few selected discrete sources.

The brightest sources in the northern hemisphere are Cassiopeia A and Cygnus A. The observed spectra of these sources are reproduced in Figure 10. The downward curvature of these spectra has been discussed by many authors and it appears that it is due to ionized hydrogen (HII regions) either in the source or in the line of sight between the source and the observer. For an electron kinetic temperature of 10^4°K, this absorption is given by

$$S(f) = S_o(f)e^{-\tau}, \quad \tau \approx \frac{0.43}{f^2} < N_e^2 L >$$

where $S(f)$ is the observed flux density; $S_o(f)$ is the flux density in the absence of absorption; τ is the optical depth; N_e is the electron density in cm^{-3} in the absorbing region; L is the path length thru the cloud in parsecs (pc); and $< N_e^2 L >$ is the integrated (square of) electron density along the path usually referred to as emission measure in units $cm^{-6}pc$. Existing data indicate that the low-frequency spectrum of Cassiopeia A can be explained as due to absorption with $< N_e^2 L > \sim 300$ $cm^{-6}pc$. The Cygnus A spectrum is similar; however, it appears that HII absorption is not the only

responsible mechanism in its low-frequency spectral behavior. It has been suggested that other phenomena such as synchrotron self-absorption or Razin effect (Ref. 12) may be important. The suggestion of synchrotron self-absorption would require that the Cygnus A radio source contain structural details with angular sizes of a few seconds of arc. The Razin effect would require the existence of a plasma cloud in front of the emitting region so that the emission is decreased through the change of refraction index in the medium. Investigations of these and other similar sources at lower frequencies would permit the determination of physical parameters pertaining to the source and the intervening medium to higher accuracy than has previously been possible.

It is common to ascribe to radio sources a parameter α known as spectral index which is defined by

$$\alpha = - \frac{d(\log \text{ flux density})}{d(\log \text{ frequency})}$$

which is the (negative) slope of the spectrum on a log-log plot. An example of a source which exhibits a linear spectral behavior down to 10 MHz is Taurus A shown in Figure 11; the spectral index for this source is $\alpha \approx 0.25$. Radio emissions from most discrete sources are believed to be due to synchrotron radiation of relativistic electrons as they spiral in a magnetic field. If the energies of these relativistic electrons are distributed with a power law of the form $N(E) = K E^{-\gamma}$, then the resultant synchrotron emission in the radio spectrum will have a spectral index

$$\alpha = \frac{\gamma - 1}{2}$$

This seems to be true in the case of our galaxy where the radio spectral index $\alpha \approx 0.6$ and where the observed index in the distribution of energy of low energy cosmic rays, $\gamma \simeq 2.2$.

As one proceeds to lower frequencies, the HII absorption should become apparent in the spectra of all discrete sources. The emitting regions should contain some ionized hydrogen; in addition, the radio radiation passing through our own galaxy will also suffer absorption due to interstellar HII. In

principle it should be possible to distinguish between the two contributions to absorption by a detailed examination of the source spectra. This knowledge would in turn contribute greatly to our knowledge of the structure of the emitting regions and of the distribution of HII in our own galaxy.

An additional class of radio sources, which seems interesting at low frequencies is the category of sources whose spectra are curved upward, for example the Seyfert galaxy NGC 1275 and the associated radio source 3C84. (see Fig. 12). These sources exhibit rather normal spectra with spectral indices of the order of 0.75 at meter wavelengths, but at lower frequencies their spectra steepen, having indices in the range 1.25 - 2. At frequencies in the 10 MHz range these sources are 3 - 10 times stronger than would have been predicted on the basis of their spectral behavior at frequencies above 100 - 200 MHz. Further, there is a tendency for the mean spectral index of all such sources to steepen with decreasing frequency (see Fig. 13). The low frequency enhancement in these sources is attributed to an extensive halo surrounding the higher frequency source; this halo is attributed to a violent explosive event which occurred some 10^7 years ago. The large number of particles released and accelerated during this explosion have now expanded and lost much of their energy by radiation and other loss mechanisms. It can be shown that a relativistic particle with energy E BeV in a magnetic field of B microgauss will radiate at radio frequencies in the vicinity of f MHz, given by the relation

$$f = 4.6\ B\ E^2$$

Since the higher energy particles lose energy by radiation faster than the lower energy particles, the initial distribution at the time of the explosion will now be modified so that lower energy particles predominate and hence the region will preferentially radiate at lower frequencies. In addition, the magnetic field strength would decrease as the region expands, with the result that B would vary as $(\text{radius})^{-1.5}$; hence, if the expansion were uniform with time, it would vary as $(\text{time})^{-1.5}$. From such considerations, it can be shown that if a spectral "kink" occurs at a frequency, f MHz, the age, t, is given by

$$t \sim 2.6 \times 10^{10}\ (B^3 f)^{-1/2} \text{years}$$

The study of radio sources with similarly curved low-frequency spectra would be of great interest since it enables us to study the evolution of these sources. It is likely that such sources are quite numerous at low frequencies, accounting for perhaps 10 - 20 percent of the sources detected to date at frequencies near 10 MHz.

Additional types of sources are likely to be discovered from observations with LOFT. For example, the Crab Nebula has been found to possess a compact low-frequency component which accounts for a large fraction of its emission at low frequencies. Although its spectrum, as shown in Figure 11, is linear down to 10 MHz, it is quite possible that this small region, which seems to have a very steep spectral index, will cause a significant low frequency enhancement at frequencies in the 1 - 10 MHz range. At the present time, the physical nature of this low-frequency component is unknown; in this respect the low-frequency observations are likely to be important. Systematic low-frequency observations could result in the discovery of more sources of similar nature; that is, exhibiting similar behavior at low frequencies.

Let us now attempt to estimate the behavior of the sky at low frequencies from our knowledge at higher frequencies. As discussed earlier, the spectral index, α , and emission measure, $< N_e^2 L >$, are related to flux density $S(f)$ by the relation:

$$S(f) \propto f^{-\alpha} \exp\left[-\frac{.43}{f^2} < N_e^2 L >\right]$$

In Figure 14 are plotted, for $< N_e^2 L > = 10$ and $100\ cm^{-6}pc$, the spectral behavior of sources with spectral indices $\alpha = 0.25$, 0.75, and 1.50 . These curves have been normalized to the 100 MHz flux density and assume that the HII absorption comes from a region between the source and observer. These particular spectral indices were chosen to be characteristic of the spectral indices of sources like supernova remnants, extragalactic sources and some peculiar extragalactic sources with curved spectra (Ref. 13).

The two emission measures chosen for illustration are $< N_e^2 L > = 10\ cm^{-6}pc$ characteristic of the mean over the whole

galaxy and $< N_e^2 L > = 100$ cm^{-6}pc which might be typical of sources having HII clouds in the line of sight. Sources with $< N_e^2 L >$ much larger than a few hundred would be relatively unimportant at 10 MHz or lower, unless the sources were very strong at somewhat shorter wavelengths. Thus we may regard the range $< N_e^2 L > = 10 - 100$ cm^{-6}pc as typical for most of the sources which would be observed in the 1 - 10 MHz range. It should be noted that for $\alpha = 0.75$ and $\alpha = 1.50$ sources have their spectral maxima in the 2 - 10 MHz range, and that for these sources, the flux density of the maxima is several times the flux density in the 10 - 100 MHz range. In Figure 15, are plotted the flux density relative to 10 MHz for frequencies $f = 3$ and 5 MHz as a function of spectral index α for $< N_e^2 L > = 10$ and 100 cm^{-6}pc. In these plots, α is measured on the unabsorbed or linear portion of the spectrum. Thus α applies at frequencies f such that $f > 2(< N_e^2 L >)^{1/2}$.

Log N-log S plots

The statistical behavior of a large number of sources is discussed in terms of a "log N - log S" plot, wherein the logarithm of the number, N , of sources brighter than a flux density, S , is plotted vs. the logarithm of the flux density. Such plots have profound cosmological significance. Consider that all sources emit energy at a rate, W watts, and that there are n sources per unit volume. The power, S , per unit collecting area received from a source at a distance, R , will then be

$$S = \frac{W}{4\pi R^2}$$

All sources brighter than S will then be contained within the sphere of radius

$$R = \left(\frac{W}{4\pi S}\right)^{1/2}$$

The total number of sources brighter than S will thus be

$$N = 4/3\ \pi\ R^3\ n = 4/3\ \pi\ n\ \left(\frac{W}{4\pi S}\right)^{3/2}$$

Expressed in logarithmic terms, this becomes

$$\log N = \log\left(\frac{4}{3}\ \pi n\right) + \frac{3}{2}\log\left(\frac{W}{4\pi}\right) - \frac{3}{2}\log S$$

This relation gives on a log-log plot, a straight line with a slope, β , of $-3/2$. One important problem of cosmology concerns the utilization of the observed β's as tests for various cosmological models of the universe.

One particular solution which is of interest to low-frequency radio astronomy is one in which a linear extinction coefficient (for example, as might be due to HII absorption) is included. Thus

$$S = \frac{W}{4\pi R^2}\ e^{-\tau}$$

where

$$\tau = kR \approx \frac{0.43}{f^2} < N_e^2 R >$$

Then the sources brighter than S will be contained within the sphere

$$R = \left(\frac{We^{-\tau}}{4\pi S}\right)^{1/2}$$

and the total number of sources brighter than S will be

$$N = \frac{4}{3}\ \pi R^3 n = \frac{4}{3}\ \pi n\ \left(\frac{We^{-\tau}}{4\pi S}\right)^{3/2}$$

from which it can be shown that

$$\beta = \frac{d \log N}{d \log S} = -\frac{3}{2}\left(\frac{2}{2+\alpha}\right)$$

And since $\tau = kR$, we see that the more distant (and hence weaker) sources contribute less power than they would in the absence of absorption so that the log N - log S plot will flatten out to $\beta = 0$ as τ increases. Estimates of log N - log S values at 5 and 3 MHz have been made (Ref. 13) on the basis of extrapolation from published data around 10 MHz. The results of such extrapolation do not lead to any definite conclusion, and consequently, it will be worthwhile to study this important cosmological problem from direct low-frequency observations.

STUDY OF RADIO EMISSIONS FROM JUPITER

The planet Jupiter is a very active emitter of radiation at radio wavelengths. As a radio emitter in the solar system, it is much stronger than the sun at frequencies around 10 MHz.

Jovian Radiation at Centimeter and Decimeter Wavelengths

Jovian radio emission at wavelengths of less than 1 meter consists of two components: (1) a thermal component which predominates at wavelengths shorter than 5 cm, the flux density decreasing approximately as the inverse square of the wavelength; (2) a steady nonthermal component which predominates at long decimeter wavelengths, with the flux density increasing toward longer wavelengths approximately as 0.3 power law. Separation of the two components is marked by a definite change of slope in spectral intensity at about 10 cm. The thermal emission is randomly polarized and appears to originate from the upper atmosphere. The nonthermal decimeter component is roughly 30% linearly polarized and about 6% circularly polarized. The electric vector of linear polarization varies cyclically from parallelism with the Jovian equatorial plane through roughly $\pm$ 10 degrees during the rotation period. At 31 cm wavelength, the angular size of Jovian radio emission is 2.9 and 1.2 times the diameter of the planetary disk in the equatorial and polar directions, respectively. It is presently believed that this steady nonthermal component is due to synchrotron radiation of relativistic electrons trapped in the Jovian radiation belts.

Jovian Radiation at Decameter Wavelengths

The Jovian radio emission at decameter wavelengths (8 to 60 meters) consists of sporadic storms whose apparent intensity can exceed that of any other radio source in the sky except the sun. The principal characteristics of these emissions can be summarized as follows:

The emission is bursty, narrow band and circularly polarized. The absolute upper frequency limit for this emission is about 40 MHz. The bursts, as observed at a single frequency, have

typical durations of 1 - 10 seconds (called L-pulses), although bursts with durations of milliseconds have been observed (S-pulses).

The emission exhibits a periodicity with the planetary rotation. The radio rotation rate differs slightly from the rotation rate inferred from optical features. A coordinate system based upon radio periods defines a central meridian longitude λ_{III} with a rotation rate of $9^h55^m29^s.37 \pm 0^s.13$. The emission characteristically drifts upward in frequency as a function of time for λ_{III} in the 0° - 180° range and downward in the 180° - 360° range.

The emission probability varies with λ_{III} and in the 20 - 30 MHz range, emission peaks occur at longitudes in the range 90° - 130° and 210° - 250°. This probability is also controlled by the position of the inner Gallilean Satellite Io (see Fig. 16). The emission probability is maximum when Io has a geocentric phase of 90° and 240° (see Fig. 17). The former region corresponds to the emission peak for λ_{III} in the 90° - 130° range. The Io control appears to be strongest when it lies in the plane λ_{III} = 20°, 200° which contains the Jovian magnetic axis.

The source of decametric bursts seems to be smaller in size than 5 - 10 seconds of arc and, in fact, it may have a much smaller size as suggested by the evidence of interplanetary scintillations of Jovian decametric radiation.

At frequencies of 10 MHz or less, the most striking feature observed is the high emission probability (50 per cent or greater) as compared to that (10 per cent or less) at higher frequencies. One observes maxima in the range 200° to 250° LCM and minima in the range 120° to 150° LCM. There seems to be a shift in the emission probability maxima and minima with a change in frequency at the rate of 16° - 18° per MHz around 10 MHz (Fig. 18).

The emission probability around 10 MHz also seems to depend strongly on the phase of Jupiter's satellite Io (see Fig. 16). The main peaks occur at Io phases of 80° and 240°. These are essentially the same angles at which enhancement occurs at higher frequencies. In addition, less intense maxima occur at 100° and 340° around 10 MHz but not at higher frequencies. Figure 19 shows (according to Ref. 14) a plot of the total emission

probability as a function of LCM and Io phase for all frequencies in the range 8 - 41 MHz. It is clear that the source at LCM = 110° - 160° and Io phase = 60° - 110° ("early" source) is very sharply defined. The "main" source at LCM = 210° - 260°, exhibits some Io control, but to a lesser degree than the early source. The "third" source at LCM = 280° - 360° is similar to the main source from the point of view of Io control. The "fourth" source which occurs at low frequencies at LCM = 10° occurs at the Io phase of 60°. This source is a precursor to the early source emission since time moves along lines parallel to the dashed lines in Figure 19. In Figure 20 is shown the corresponding plot at 9 MHz. Here the prominent features of the higher frequency plots are missing. The "fourth" source is the only one which appears clearly in the low frequency plot. It should be noted that the low frequency plot is not as accurate as the higher frequency plot, because of insufficient data. However, these plots suggest that Io does not exert a strong control over the emission at frequencies of 10 MHz or less, in contrast to the very strong control, particularly in the early source region, exhibited at frequencies in the 20 - 40 MHz range.

As mentioned earlier, the emission probability at low frequencies of 10 MHz or less is much higher than at higher frequencies. At higher frequencies one can predict favorable conditions for Jovian emission from considerations of Jupiter - Io geometry. At lower frequencies the emission appears to occur almost all the time. This observation has resulted in the suggestion that the emission at low frequencies tends to a continuum. This emission is often very weak and it has a wideband, continuous and constant character. This emission may be a true continuum with some variability attributable to interplanetary and ionospheric scintillations. Alternatively, it may simply be the effect of merging of many weak bursts. It seems that dynamic spectra with high time resolution will help understand the true nature of this emission.

A possible power spectrum of Jovian decametric continuum estimated by Clark (Ref. 13) is shown in Figure 21. It should be noted that the general character of the Jovian radiation is narrow-band and bursty. The points calculated by Ellis (1965) represent only the time-averaged power and do not represent the high instantaneous value or narrow-band character of an individual burst. The 10 MHz continuum flux density represents the minimum observed Jovian flux density. Thus, at low frequencies one often

observes an apparent continuum emission from Jupiter, which is punctuated by bursts having intensities much higher than the continuum level.

The dynamic spectrum observations have proved to be extremely valuable for the study of temporal and frequency characteristics of Jovian bursts. Thus, the frequency-time characteristics appear to be fixed in the system III coordinates, and the combined Io phase and system III LCM geometry seem to control the spectral behavior of the signals having time scales of minutes to hours. Spatial structure is also observed in the Jovian bursts, that is, the temporal variations when observed at two well separated stations are correlated, but exhibit a shift in time. This behavior is attributed to scintillations of the Jovian radiation caused by electron density irregularities in the interplanetary medium. The irregularities of electron density act as a random diffracting screen and cause scintillations of radio waves coming from a source of small angular size (typically less than 1 sec of arc). From observations at spaced stations it is found that the individual Jovian bursts have bandwidths between 100 Khz and 1 MHz, that is, between 1 and 10 per cent at frequencies around 10 MHz. This bandwidth is either intrinsic to the emission mechanism, or it may be imposed by the medium between the source and the observer, that is, by interplanetary scintillations.

Generating Mechanisms of Jovian Decametric Radiation

Since the intensity of decametric radiation is very high, often exceeding an equivalent temperature of 10^{12}°K, and the radiation is very bursty, it seems that any emission mechanism must require coherent radiation of an aggregate of particles. Various coherent mechanisms have been proposed, most of which involve radiation near the ambient gyrofrequency, arising from the interaction of a stream of particles with the ambient plasma. The control of Io on the Jovian radiation is again attributed to some kind of interaction between Io and charged particles in the vicinity of Io's orbit. The exact nature of this interaction is not known; suggestions include the generation by Io of Alfven waves in the Jovian magnetic field, physical collisions between Io and charged particles, the "tweaking" of some of the Jovian field lines by Io, the interaction between a magnetic field surrounding Io with the Jovian field, etc. The frequencey drift structure which rotates with the planet in system III coordinates

has been attributed to an offset and tilted magnetic field; the drift seems to have a symmetry about system III longitude = 200°, and to that longitude is attributed a Jovian magnetic pole; that is, the plane containing the magnetic poles and the rotational axis passes through 200° longitude. As a working model, one can imagine that as Io rotates in its orbit, it causes a stream of particles to be precipitated from the magnetosphere into the lower ionosphere of Jupiter. The stream reaches a region where the stream-plasma interaction takes place and radiation occurs at the local gyrofrequency. Since the field is symmetrical with the rotational axis, the ambient gyrofrequency changes as the planet rotates. The low frequency continuum may, at the same time, arise from a continuous non-Io controlled precipitation of particles from the magnetosphere.

An alternative model involves a magnetosphere which co-rotates with the planet, dragging charged particles along. Since the particles have appreciable angular velocity, they experience both gravitational (inward) and centrifugal (outward) forces. These forces balance at about 2.3 Jovian radii; inside this region they are distributed with a gravitational scale-height and outside this region they are thrown outward and form a flattened disk. This model would require radiation at or near the plasma frequency in the magnetosphere unlike the gyrofrequency models discussed earlier.

Possible Low-Frequency Studies of Jovian Bursts

As in the case of the sun, two kinds of measurements have contributed significantly to the understanding of Jovian physics. These are the swept-frequency (continuous spectrographic) measurements and polarimetric measurements, respectively, and there is every reason to believe that these types of data, taken at very low frequencies from space may represent both a feasible and important goal for the LOFT program. Similarly, interferometry should be used to establish source positions and angular sizes of Jovian low-frequency emission.

Jovian radio emission has not been observed below 4 MHz, where the emission has characteristics suggesting it may be occurring at the gyrofrequency in Jupiter's magnetosphere. At that frequency the emission occurs near the inner edge of the region from which the microwave radiation produced in Jupiter's

radiation belts apparently originates; the decametric emission may also continue on down to frequencies corresponding to points near the outer edge of the observed radiation belts (Ref. 15). If so, the nominal lower limit of the emission should lie below 1 MHz.

The measurement of flux density at low frequencies and the consequent determination of the overall shape of the intensity spectrum of Jovian decametric emission are of fundamental importance for the interpretation of this radiation. As discussed earlier, there seems to be a sharp cut-off at about 40 MHz and the average intensity and probability of occurrence increases as frequency decreases down to the low frequency limit of about 10 MHz imposed by the terrestrial ionosphere. The extension of this spectrum to frequencies as low as about 1 MHz would be of great use to our understanding of the emission mechanism and the spectrum of energetic particles responsible for the emission. One of the difficulties of radio noise measurements at low frequencies from a space vehicle in earth's orbit is due to the fact that in the vicinity of the earth the radio frequency environment is often dominated by frequent, intense solar radio bursts and noise generated in the terrestrial magnetosphere. However, one of the important technical features of the LOFT will be the back-lobe suppression which presently does not exist in the simple aerial systems of Radio Astronomy Explorers. Consequently, one will be able to measure the intensity of Jovian radio emission at low frequencies with much better accuracy than ever done before from a space craft. By making intensity measurements over the range 1 MHz to 20 MHz, we can extend the Jovian radio spectrum to the range of frequencies not observable from earth, study its dependence on planetary rotation and position of Jovian satellite Io, as well as provide continuity with simultaneous ground-based observations.

As discussed earlier, the Jovian decametric radiation has a long period modulation due to the planet's rotation and the position of its satellite Io. In addition, this radiation shows temporal variations on a much shorter time scale. These short time variations are mainly caused by scintillations due to the ionosphere and the interplanetary medium, and may partly be due to some basic temporal structure intrinsic to the source itself. One principle advantage of observations from space vehicles is that the effects of the terrestrial ionosphere are eliminated. This situation is particularly important since at present there

is no precise way of separating the low-frequency component of the scintillation spectra due to the interplanetary medium from that due to the ionosphere, especially when observations are made at or below 20 MHz. In addition, the "thin screen" theory of interplanetary scintillation predicts very low frequencies in the scintillation power spectra, which have never been observed. In any case, the low frequency interplanetary scintillation observations of Jovian radiation on a routine basis are likely to provide valuable information on the interplanetary medium and its behavior with activity on the sun.

REFERENCES

1. Schuerch, Hans U., and Hedgepeth, John M.: Large Low-Frequency Orbiting Radio Telescope, NASA CR-1201, October 1968.

2. Wild, J.P., Smerd, S.F., and Weiss, A.A.: Ann. Rev. Astron. Astrophys., vol. 1, p. 291, 1963.

3. Kundu, M.R.: Solar Radio Astronomy, John Wiley-Interscience Publishers, 1965.

4. Wild, J.P., et al, Proc. Astron. Soc. Australia, vol. 1, p. 79, 1968.

5. Stone, R.G., Proc. Symposium on Plasma Instabilities in Astrophysics (in press), 1969.

6. Malitson, H.H., and Erickson, W.C.: Ap. J., vol. 144, p. 337, 1966.

7. Allen, C.W.: Monthly Notices Roy. Astr. Soc., vol. 107, p. 426, 1947.

8. Ingham, M.F.: Monthly Notices Roy. Astr. Soc., vol. 122, p. 157, 1961.

9. Hartz, T.R.: Ann d'Astrophys., vol. 27, p. 831, 1964.

10. Kundu, M.R., and Haddock, F.T.: Nature, vol. 186, p. 610, 1960.

11. Ramaty, R., and Lingenfelter, R.E.: Solar Physics, vol. 5, p. 531, 1968.

12. Ginzburg, V.A., and Syrovatskii, S.I.: Cosmic Magnetobremsstrahlung, Ann. Rev. Astron. Astrophys., vol. 3, p. 297, 1965.

13. Clark, T.A., Astronomical Observations at Low Radio Frequencies, Ph.D. Thesis, University of Colorado, 1967.

14. Dulk, G.A., Science, vol. 148, p. 1555, 1965.

15. Warwick, J.W., Ann. Rev. Astron. Astrophys., vol. 2, p. 1, 1964.

References (cont'd)

16. Erickson, W.C., and Cronyn, W.M.: The Spectra of Radio Sources at Decametric Wavelengths, Astrophys. J., vol. 142, p. 1156, 1965.

17. Terzian, Y., Mezger, P.G., and Schraml, J., Astrophysical Letters, vol. 1, p. 153, 1968.

18. Wild, J.P., Physics of Solar Flares, AAS-NASA Symposium (ed. W. N. Hess), 1963.

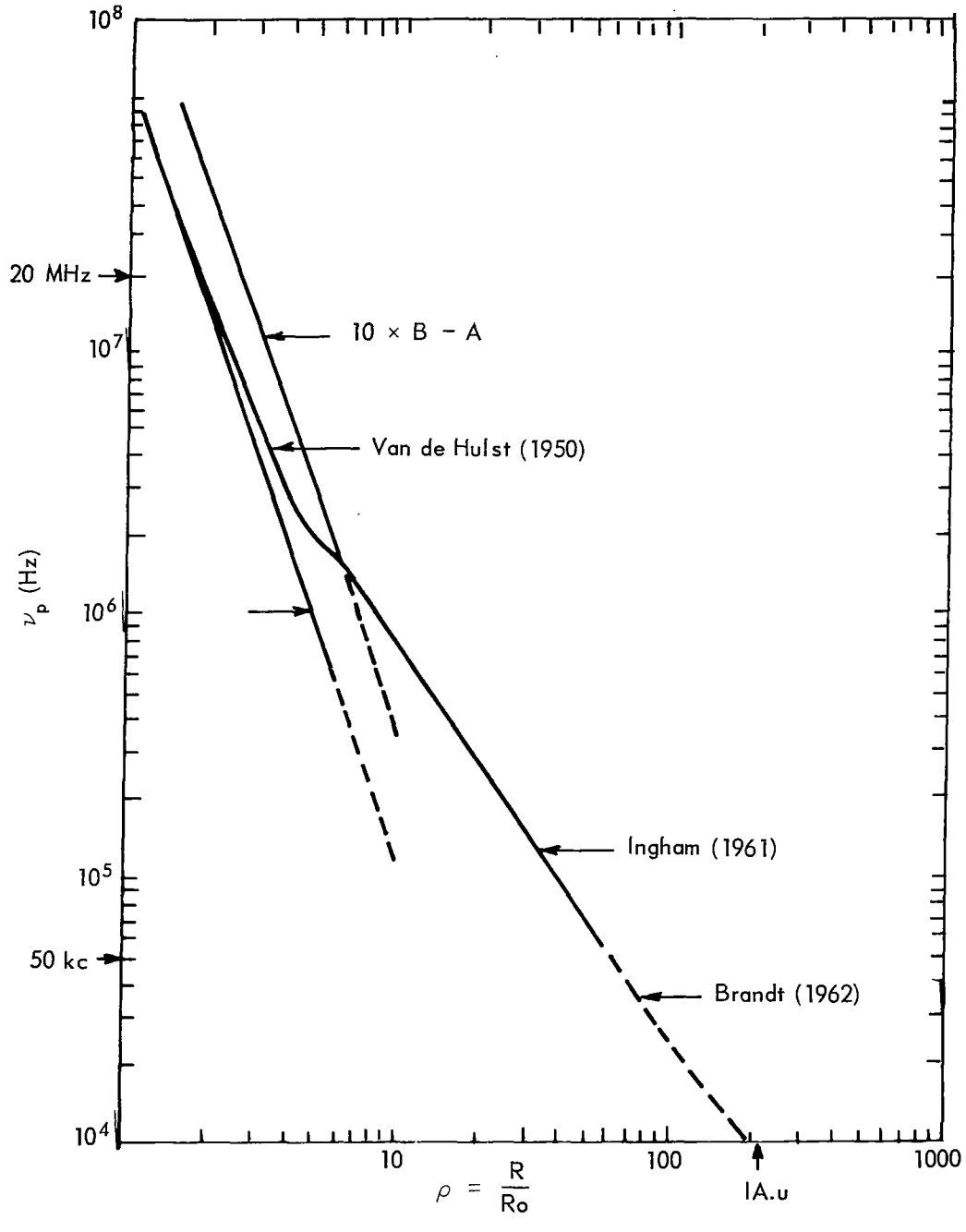

Figure 1. Plasma Frequency in the Extended Solar Corona

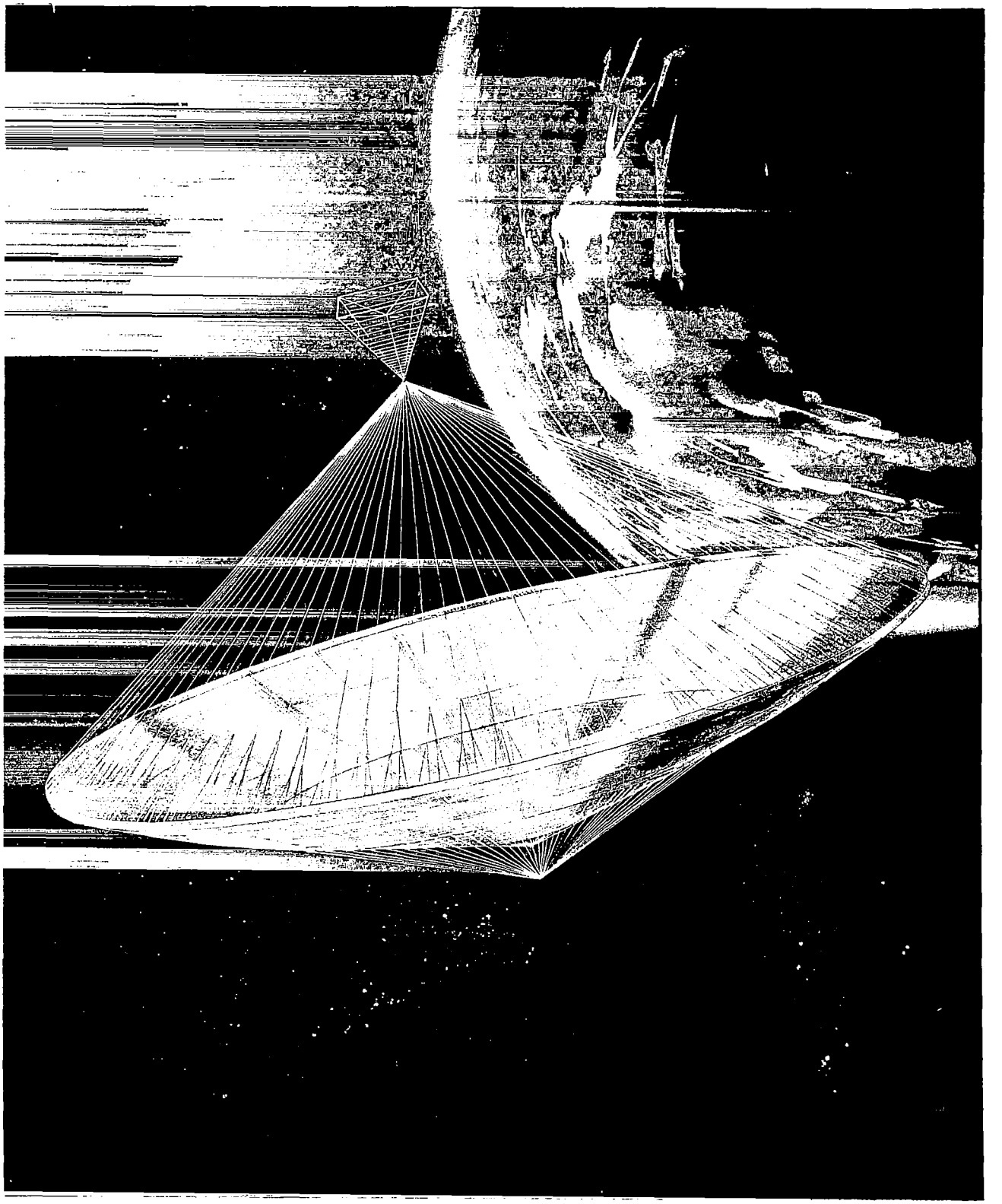

Figure 2. LOFT Baseline Concept

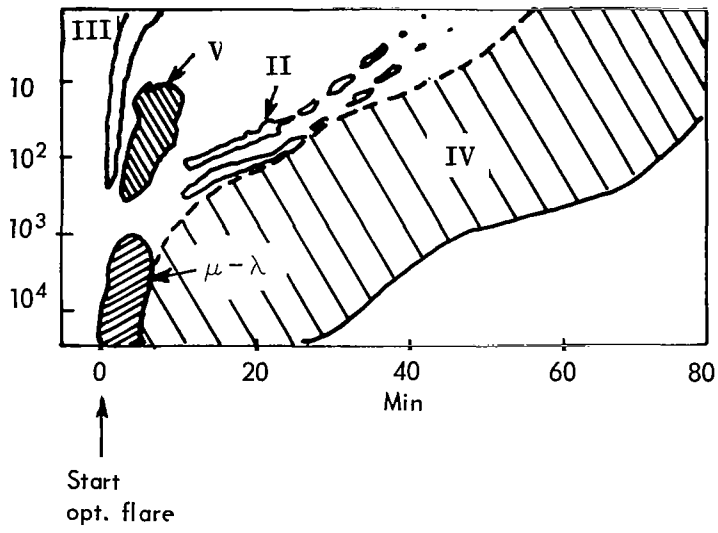

Figure 3. Typical Dynamic Spectra of Radio Bursts in the Range of Frequencies 20,000 to 1 MHz

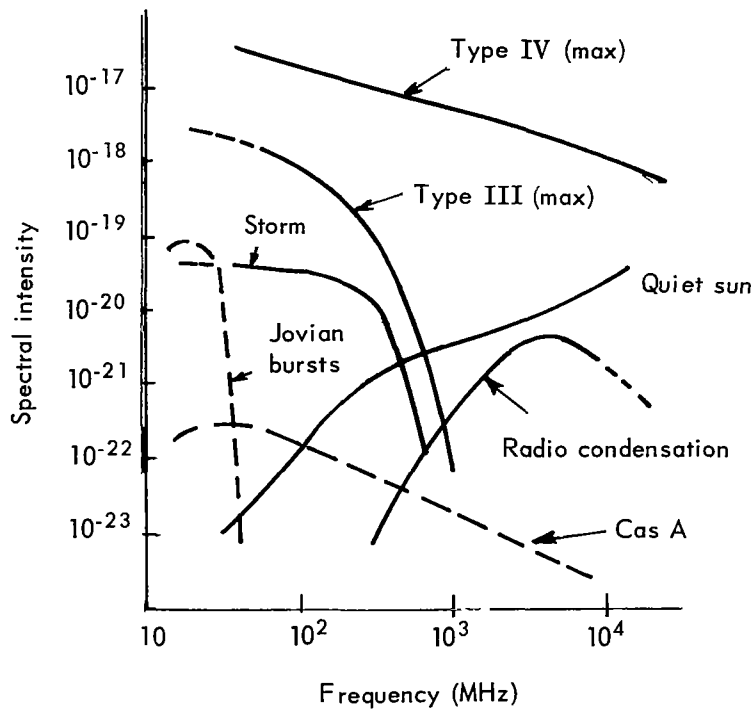

Figure 4. Power Spectra of Strong Radio Bursts Compared to Those of the Quiet Sun, Slowly Varying Component, Jovian Bursts and Cas A

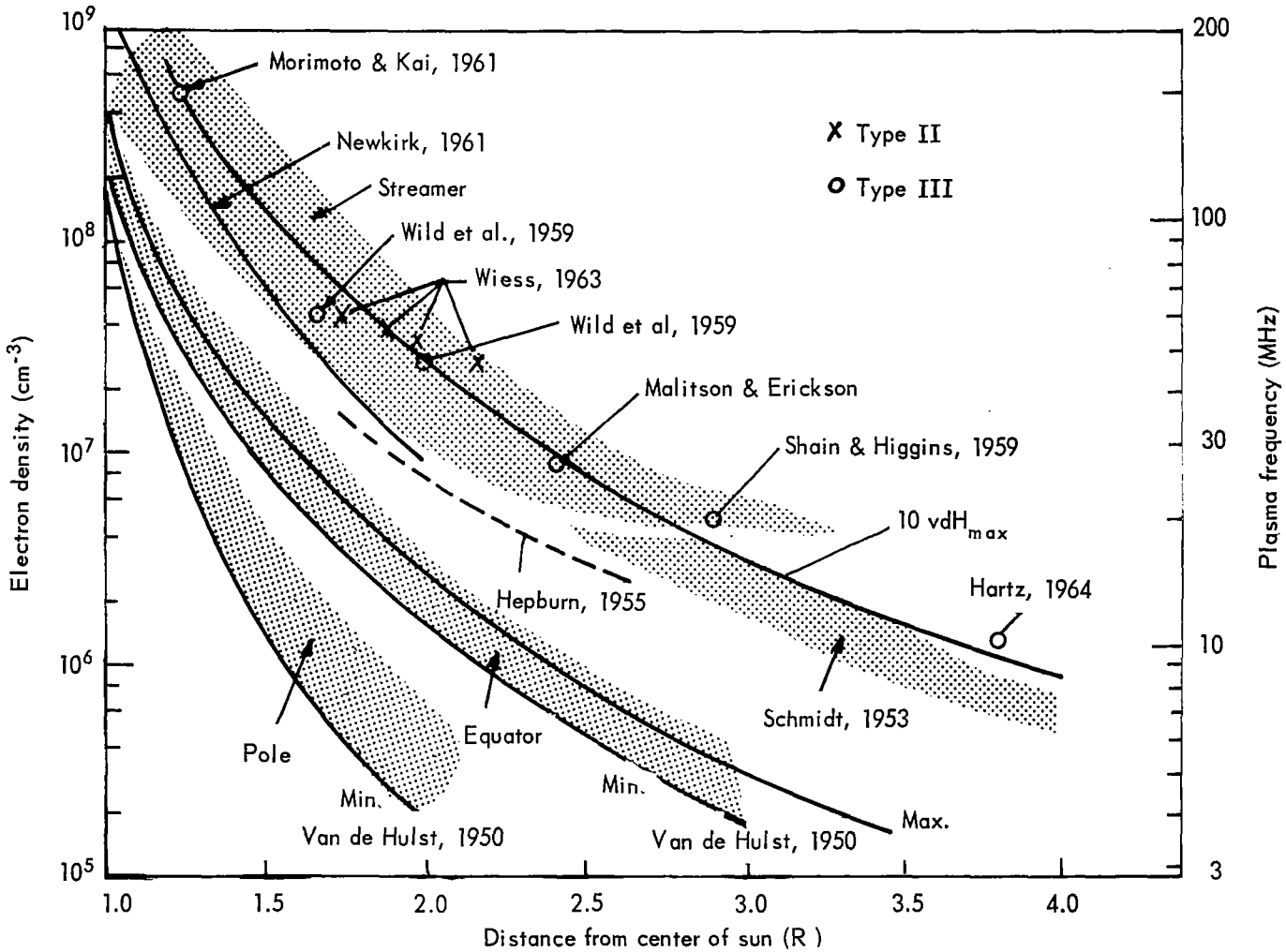

Figure 5. Estimates of the electron density distribution in the solar corona determined by various methods. The shaded areas for the polar and equatorial distributions represent results from optical eclipse observations. The solid curves are the models of van de Hulst. Optical results from streamers are shown by Newkirk's model (solid curve) and eclipse measurements of Hepburn (dashed curve) and Schmidt (shaded area). The estimates from type II and III bursts at frequencies of 10 – 201 MHz are shown by the crosses and dots and the large shaded area around them (to indicate the experimental error). The solid curve through this area is the equatorial maximum model of van de Hulst multiplied by a factor of 10 (Malitson & Erickson 1966).

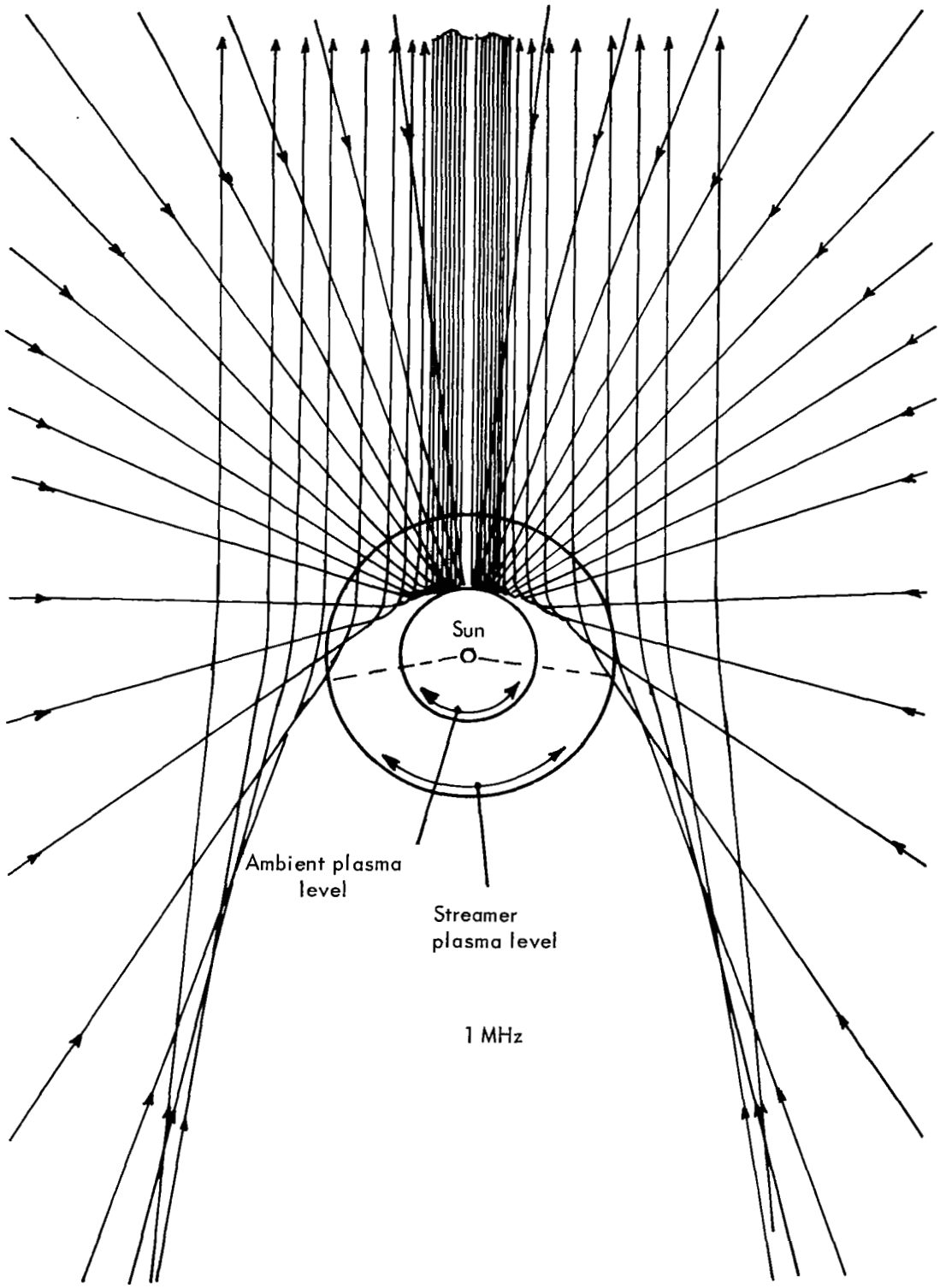

Figure 6. Ray Paths in the Solar Corona at 1 MHz, Assuming Certain Electron Density Distributions (see Text).

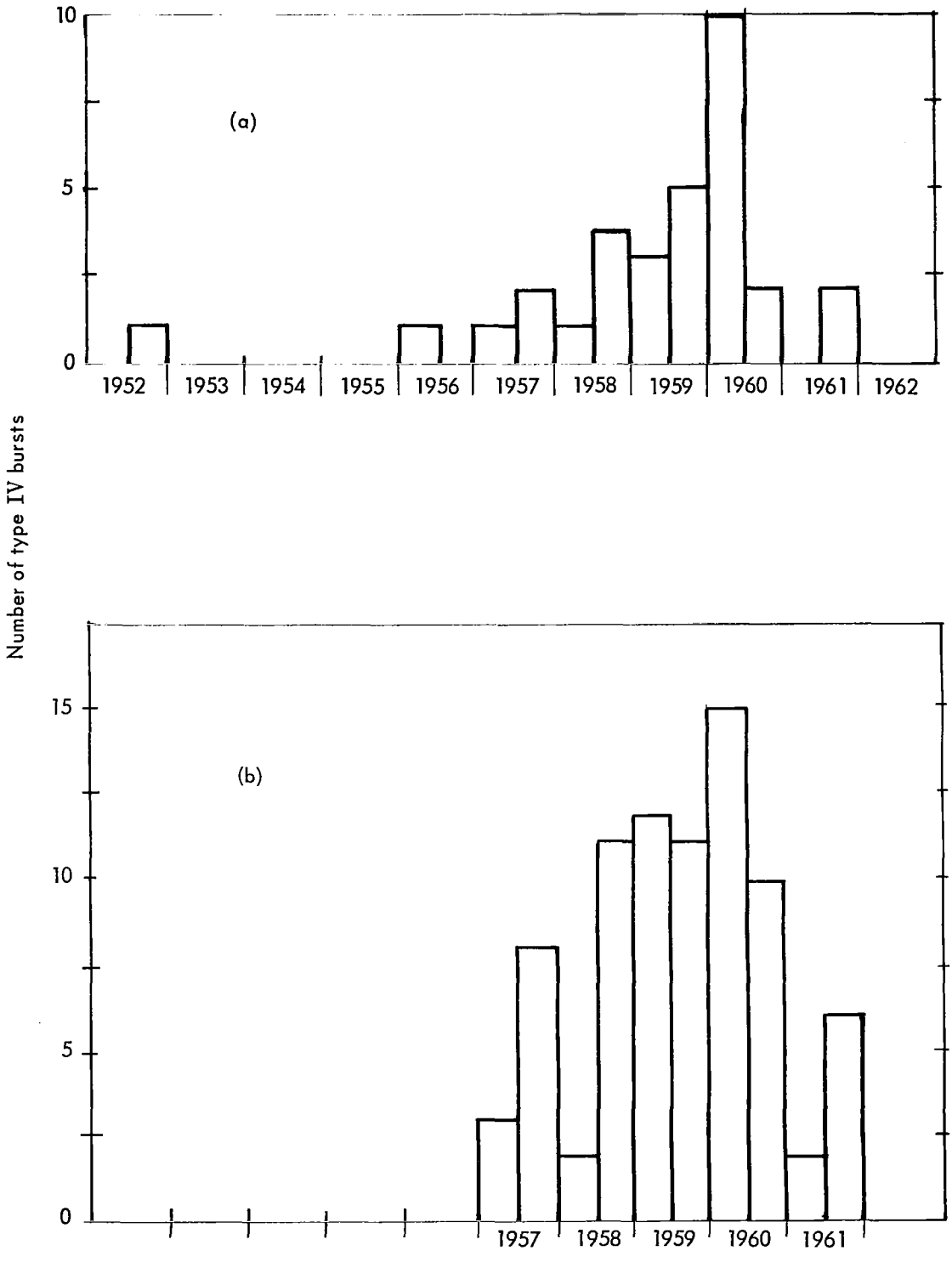

Figure 7. Occurrence of Type IV Bursts on Meter and Decimeter Waves as a Function of the Solar Cycle. (a) 25 to 240 MHz Data of Sydney; (b) 100 to 580 MHz Data of Michigan and Fort Davis.

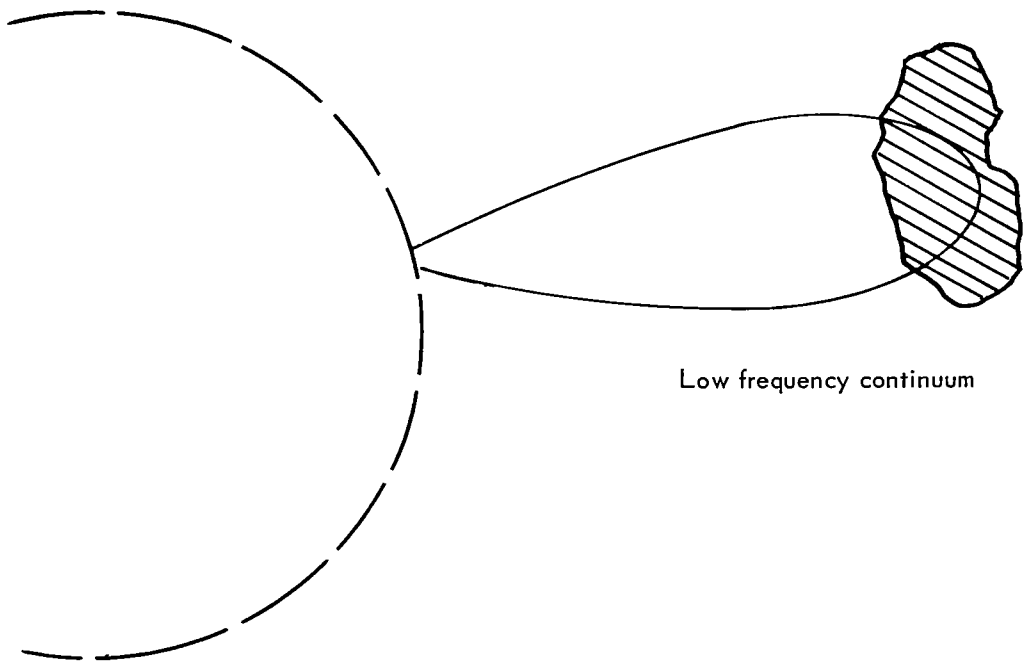

Figure 8. A Schematic of the Position of Storm Continuum at Low Frequencies

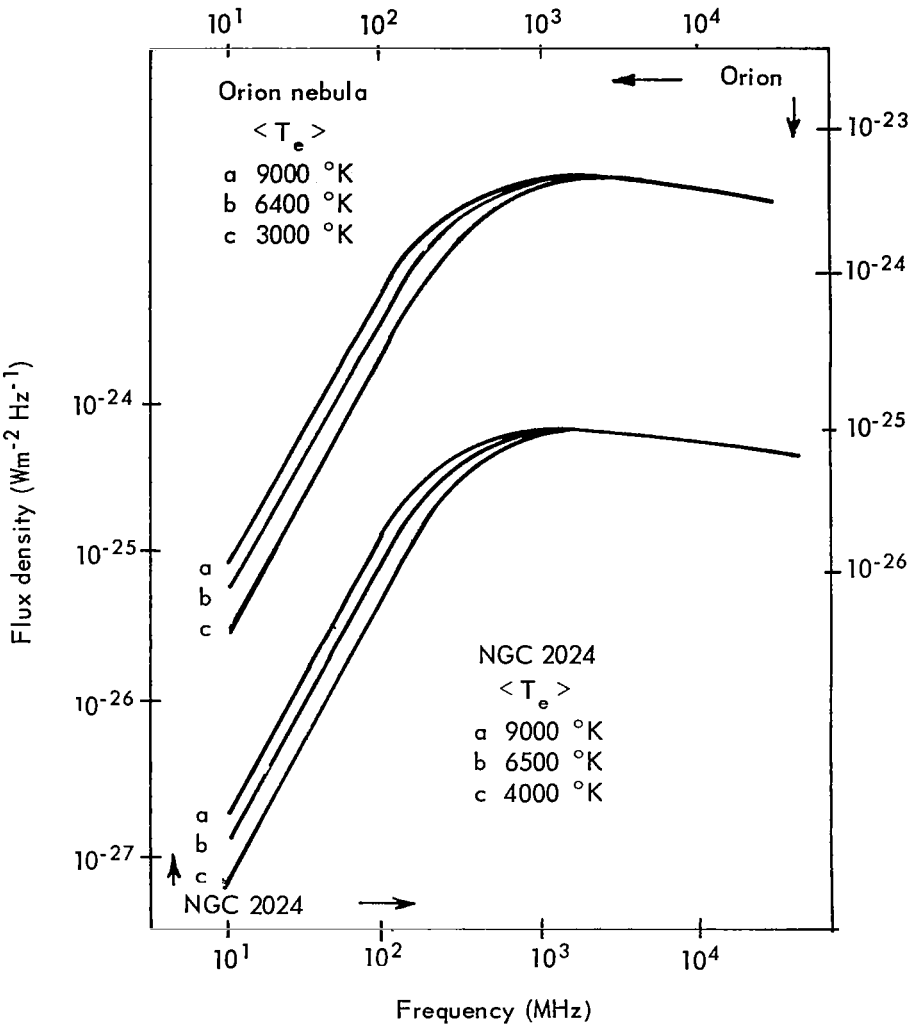

Figure 9. The Theoretically Computed Radio Spectra for the Orion Nebula and NGC 2024, Together with the Observed Flux Densities

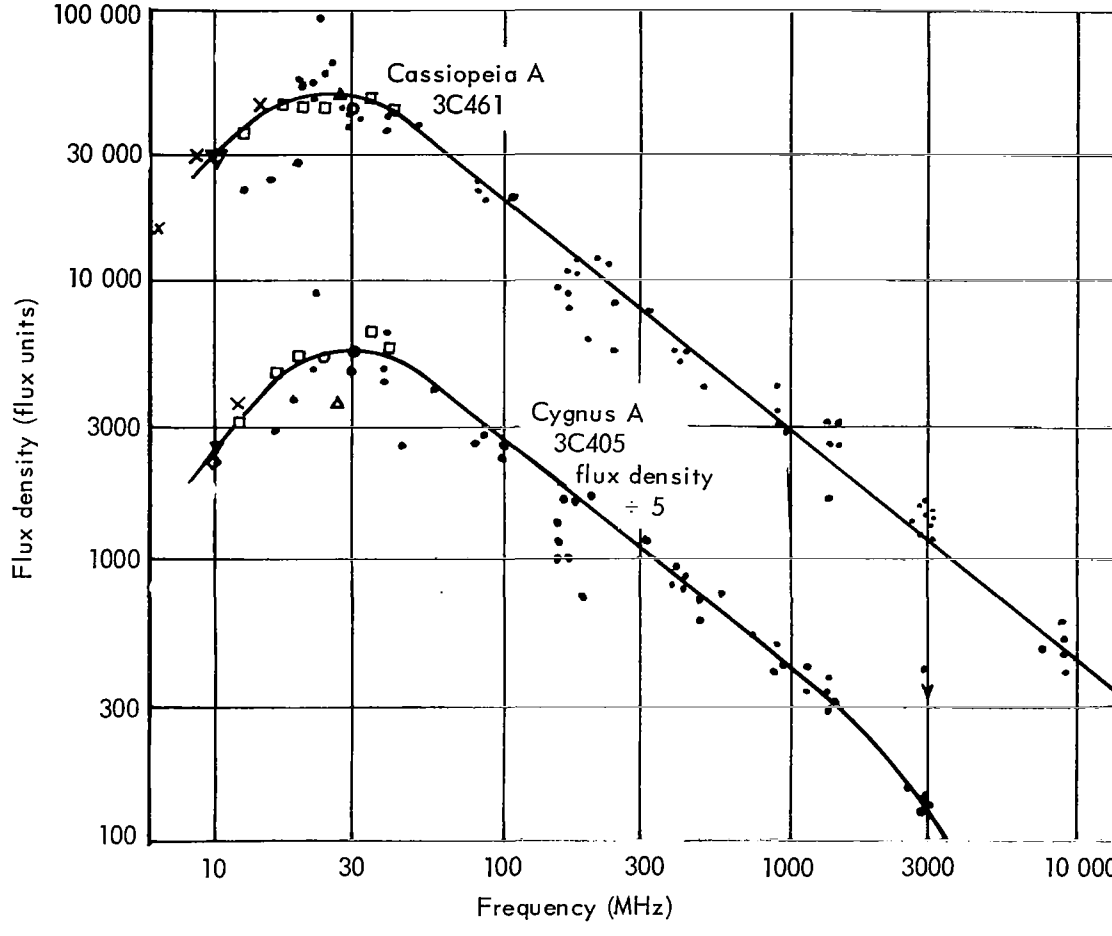

Figure 10. Spectra of the Radio Sources Cassiopeia A and Cygnus A.

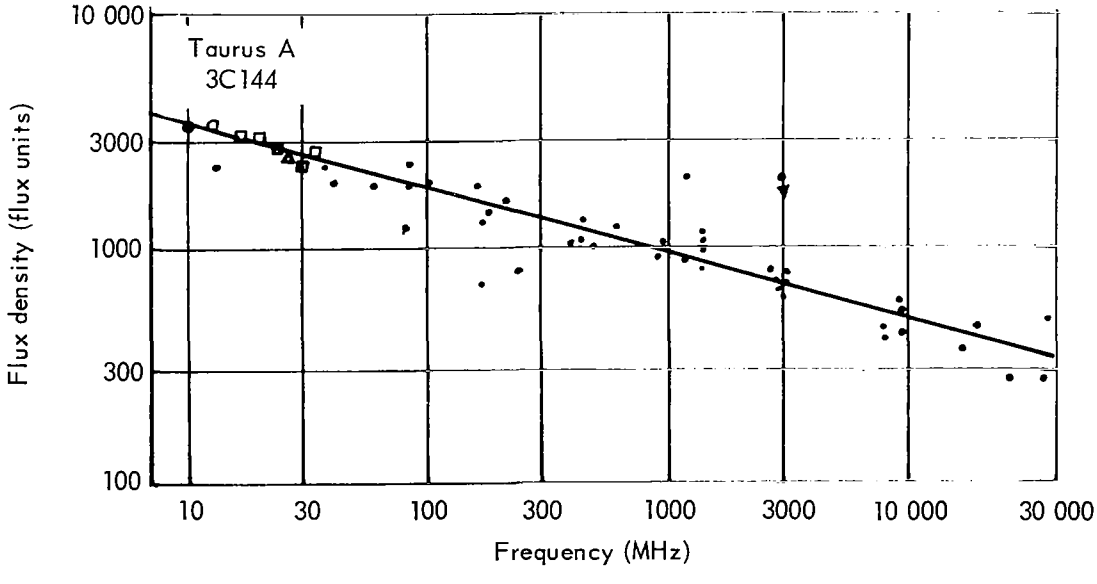

Figure 11. Spectrum of the Radio Source, Taurus A.

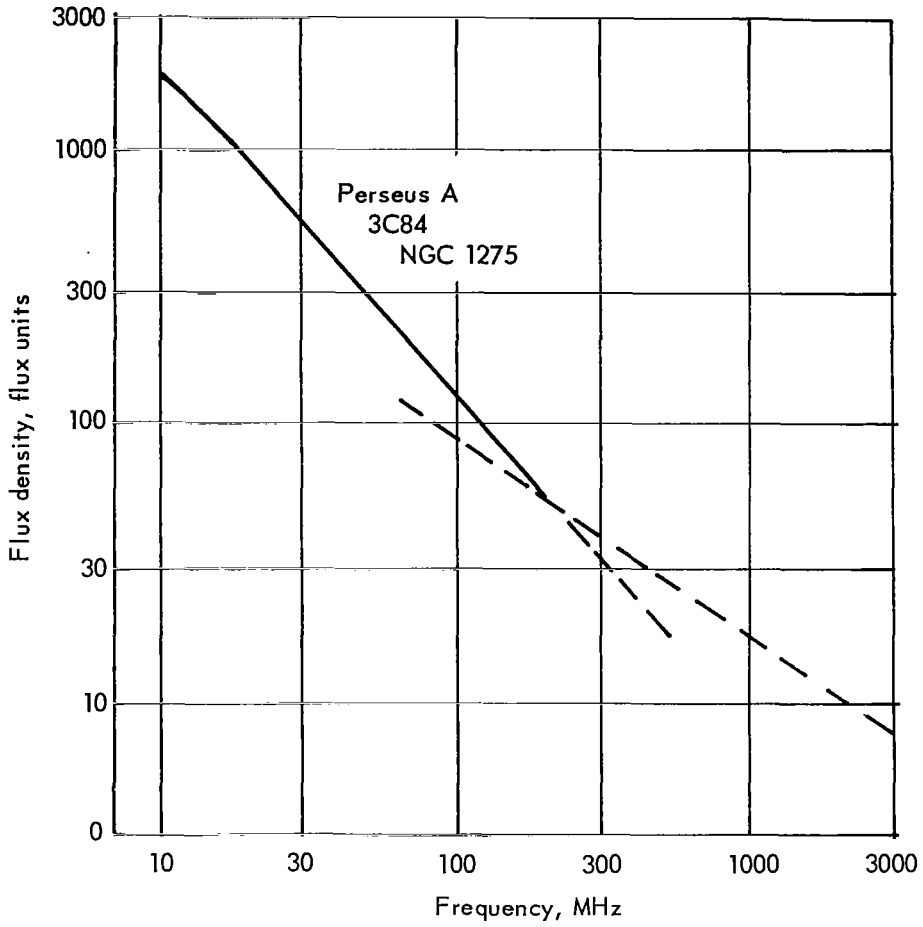

Figure 12. Spectrum of the Source 3C84 (NGC 1275)

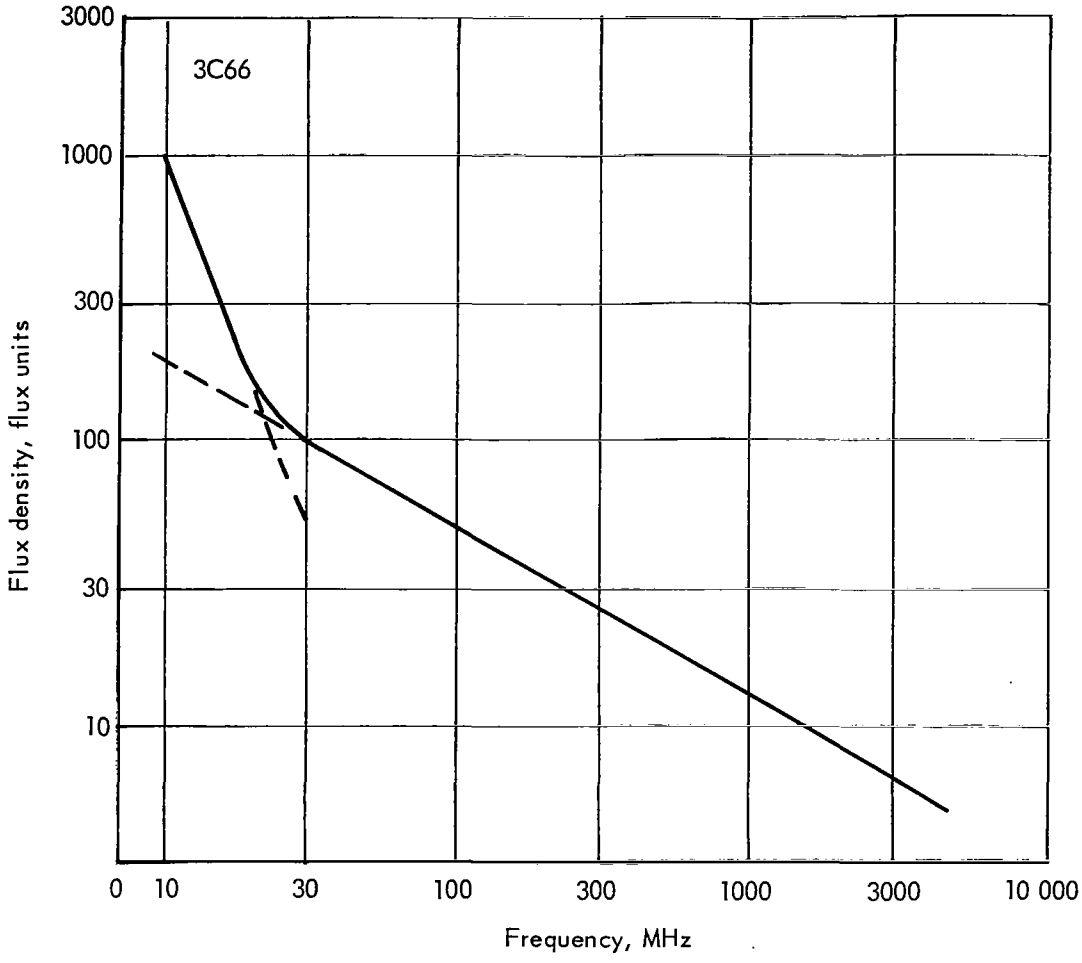

Figure 13. Spectrum of the Source 3C66

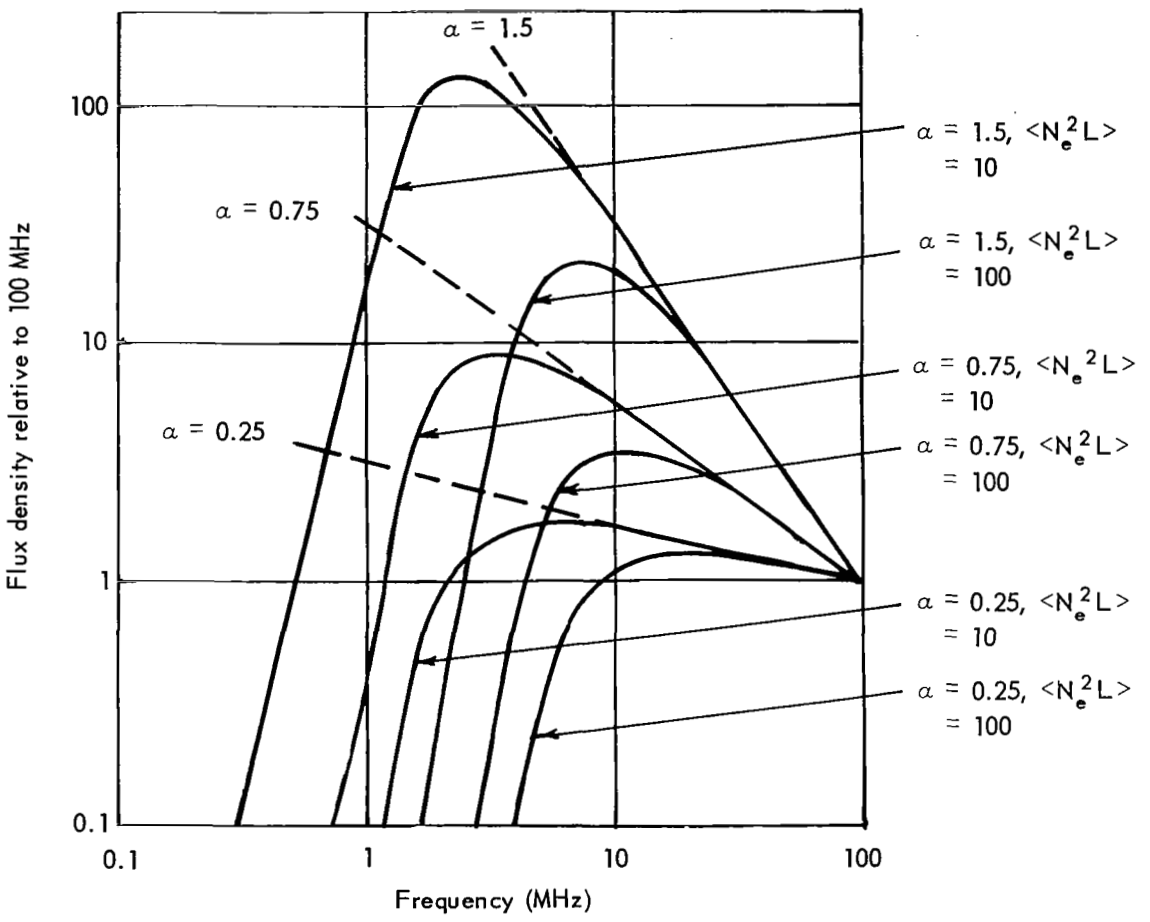

Figure 14. Examples of Radio Source Spectra with Different Spectral Indices α and HII Absorption $< N_e^2 L >$

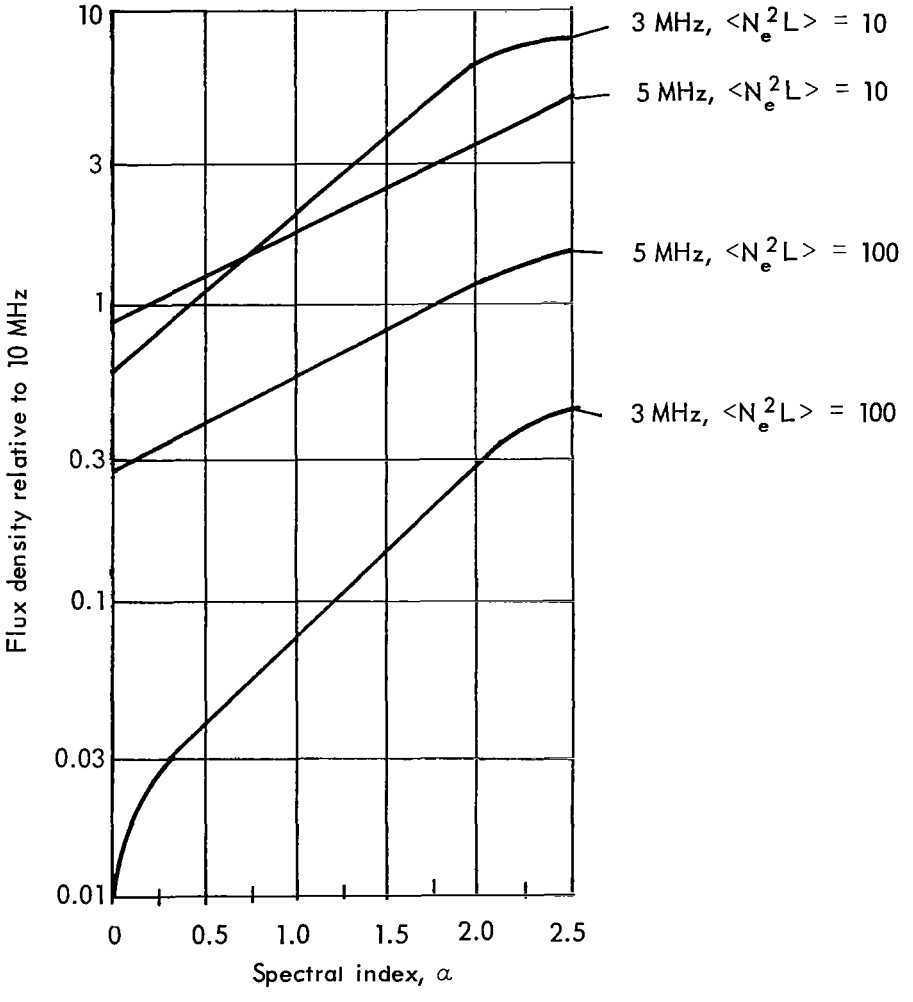

Figure 15. Flux Density Computed at 3 and 5 MHz Relative to That at 10 MHz, as a Function of Spectral Index

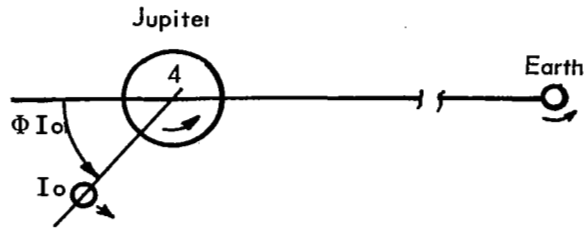

Figure 16. I_o-Jupiter-Earth Geometry

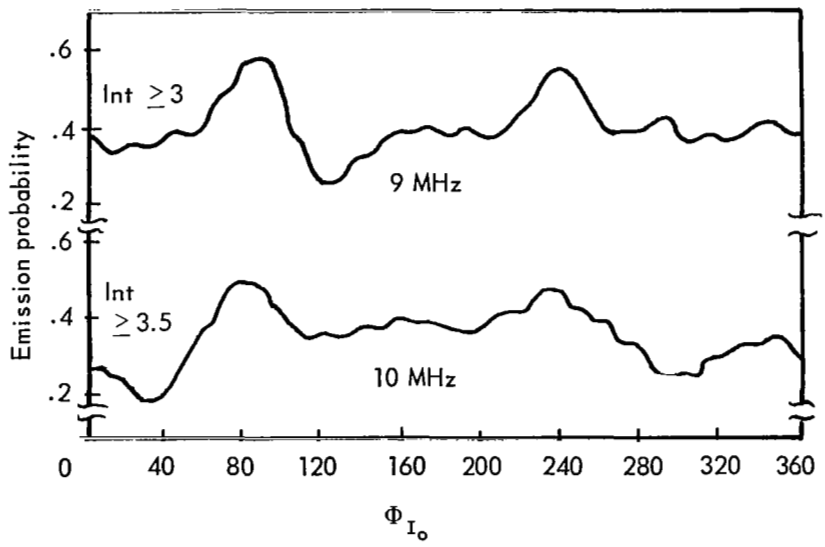

Figure 17. Dependence of Emission Probability at 10 and 9 MHz on I_o Phase

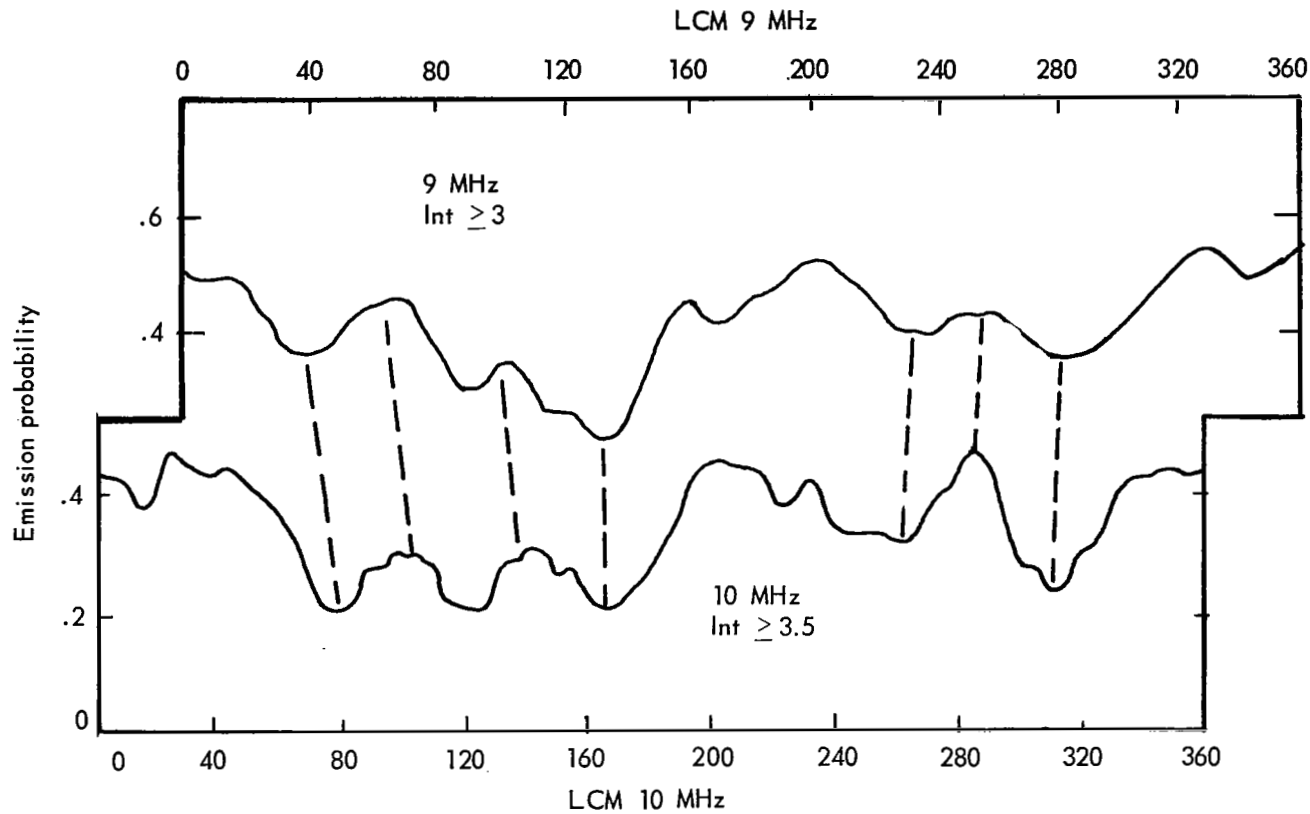

Figure 18. Comparison of the Dependence of 10 MHz and 9 MHz Emission Probability on LCM

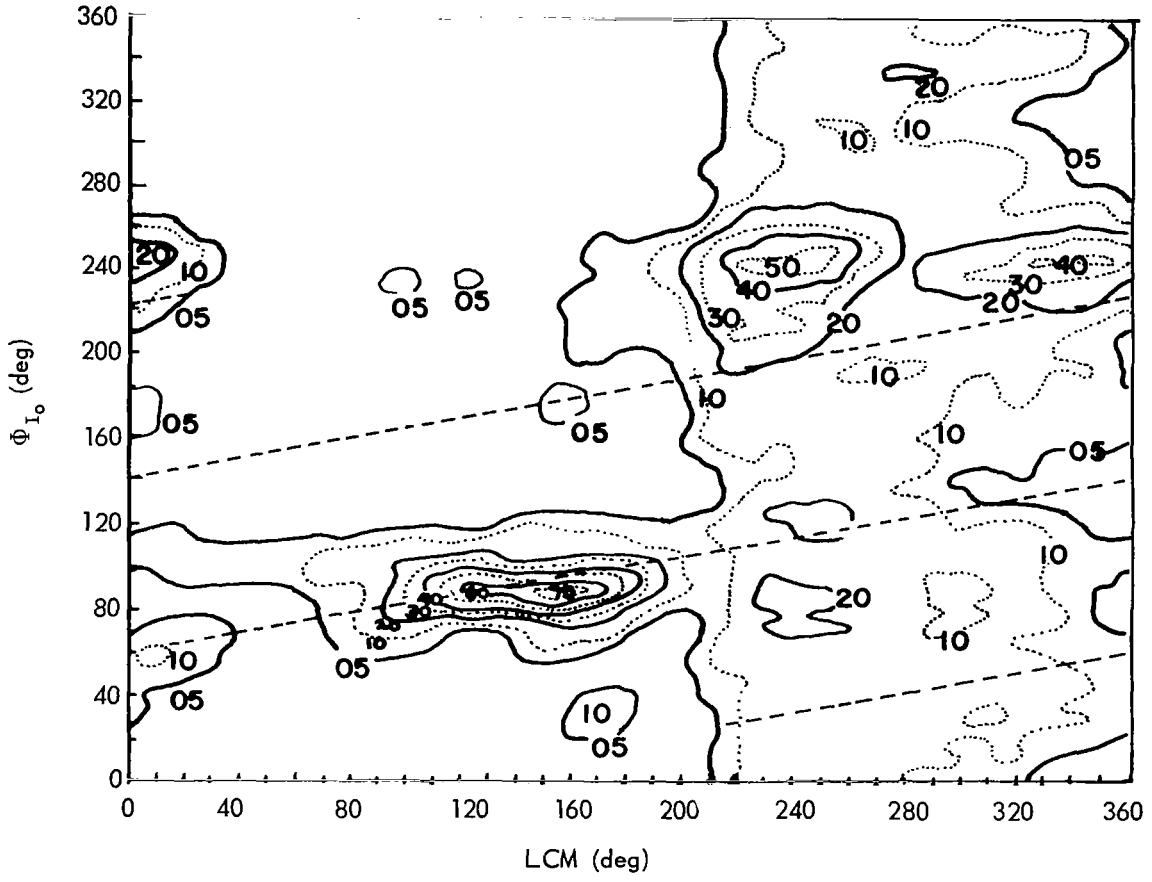

Figure 19. Plot of Joint Emission Probability as a Function of LCM and I_o Phase for all Frequencies Observed by the 7.6–41 MHz Boulder Spectrograph. (After Ref. 14.)

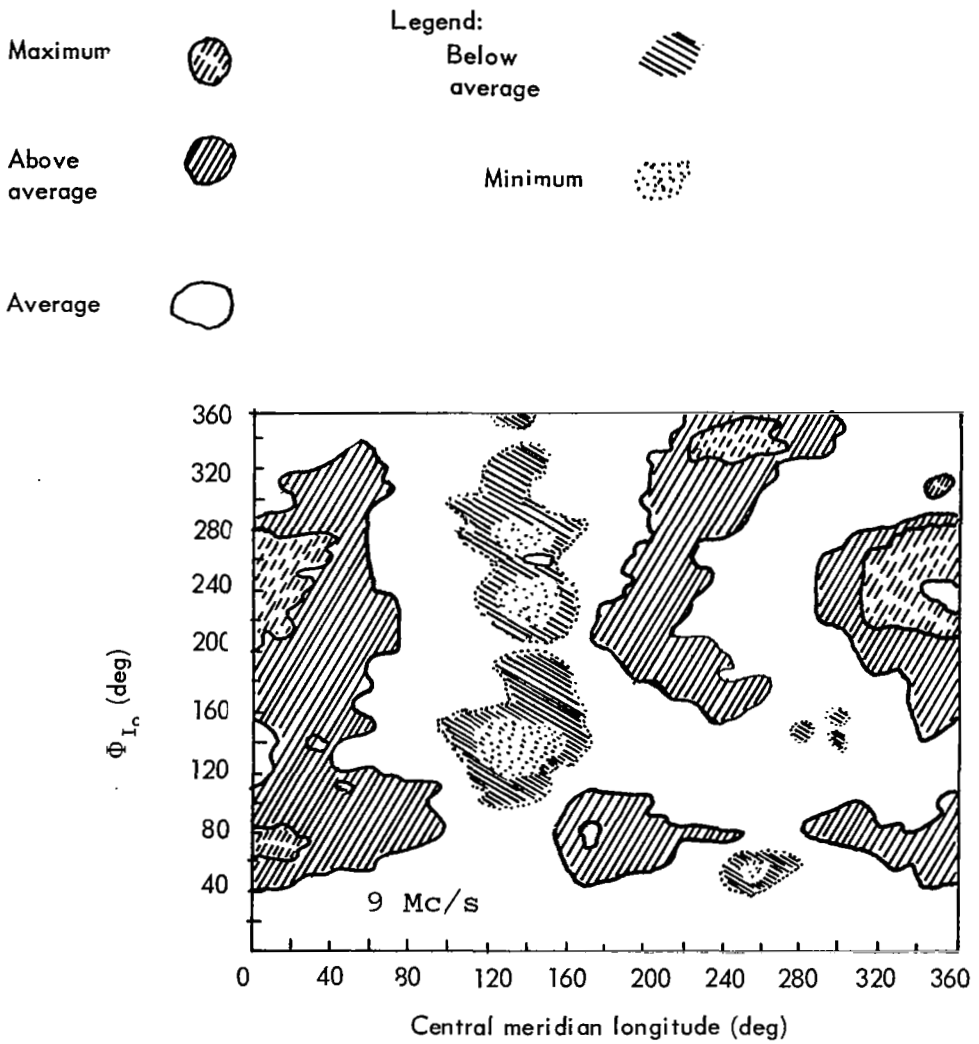

Figure 20. LCM–Io Phase Joint Emission Probability Distribution at 9 MHz.

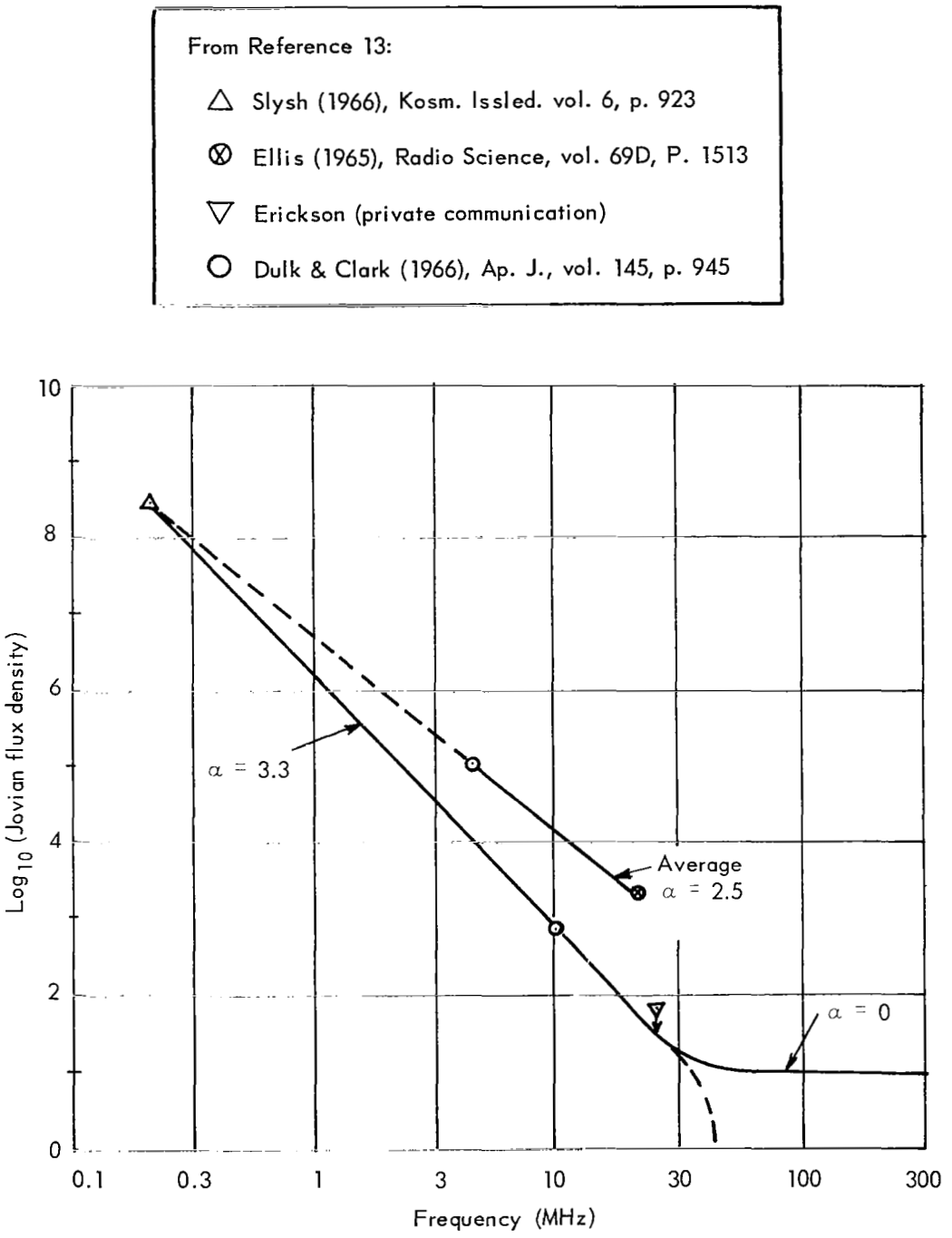

Figure 21. Possible Spectrum of Jovian Decametric Continuum Radiation